Supplementary Information

Aliphatic polycarbonates with acid degradable ketal side groups as multi-pH-responsive immunodrug nanocarriers

Adrian V. Hauck[1], Patric Komforth[2], Jessica Erlenbusch[3], Judith Stickdorn[2], Krzysztof Radacki[4], Holger Braunschweig[4], Pol Besenius[3], Simon Van Herck[5], Lutz Nuhn[1,*]

1: Chair of Macromolecular Chemistry, Institute of Functional Materials and Biofabrication, Julius-Maximilians-Universität Würzburg, 97070 Würzburg, Germany

2: Max Planck Institute for Polymer Research, 55128 Mainz, Germany

3: Department of Chemistry, Johannes-Gutenberg-Universität Mainz, 55122 Mainz, Germany

4: Institute for Sustainable Chemistry and Catalysis with Boron, Julius-Maximilians-Universität Würzburg, 97074 Würzburg, Germany

5: Meinig School of Biomedical Engineering, Cornell University, Ithaca, NY, 14850, USA

**corresponding author Prof. Dr. Lutz Nuhn*

(lutz.nuhn@uni-wuerzburg.de)

EXPERIMENTAL PROCEDURES

Materials

All chemicals were purchased commercially and, unless otherwise noted, used without further purification. 1,8-Diazabicyclo[5.4.0]undec-7-ene (DBU) and dichloromethane (DCM) were dried over CaH_2 and distillated before use. Solvents (HPLC grade) were purchased from Sigma Aldrich, Acros Organics or Thermo Fisher Scientific. Deuterated solvents were obtained from Deutero, Sigma Aldrich or Thermo Fisher Scientific. Silica for column chromatography was obtained from Machery-Nagel (particle size: 0.063 - 0.2 mm). Thin layer chromatography plates with fluorescent indicator F254 were purchased from Merck.

Nuclear magnetic resonance spectroscopy

^{1}H, ^{13}C, 2D NMR spectra were recorded at room temperature on a Bruker Avance III 300 MHz, Bruker Avance III 400 MHz, or Bruker Avance III 700 MHz FT NMR spectrometer. The chemical shifts (δ) are given in parts per million (ppm) relative to TMS. NMR spectra were evaluated with the software MestReNova 14.0.1-23559 by Mestrelab Research S. L. Samples were prepared in respective deuterated solvents and their corresponding signals referenced to residual non-deuterated solvent signals. Diffusion ordered Spectroscopy (DOSY) were recorded at room temperature on a Bruker Avance II 700 MHz FT NMR spectrometer and processed using Bayesian DOSY Transformation (minimum: 1.00×10^{-8}; maximum: 1.00×10^{-4}, resolution factor: 1.00; repetition factor: 1; points in dimension: 64).

Size exclusion chromatography

Gel permeation chromatography (GPC) was performed with THF as eluent. The sample concentration was 1–2 mg/mL. Measurements were performed at a flow rate of 1.0 mL/min at a temperature of 30 °C. As column material pol(styrene-co-divinylbenzene) (particle size: 10 µm, pore size: 500 Å + 104 Å + 106 Å, obtained from Polymer Standards Service GmbH Mainz, Germany) was used. Detection was performed by IR-detection (Agilent 1260 Infinity RID) and UV-detection (Agilent 1260 Infinity VWD). A polystyrene standard was used for the calibration (Polymer Standard Service GmbH Mainz, Germany). Toluene was used as an internal standard for the calculation of the molecular weight. The analysis of the elugram was performed using PSS-WinGPC UniChrom by Polymer Standards Service GmbH Mainz, Germany. Visualization of the data were performed using GraphPad Prism version 5.02.

Mass spectrometry

ESI mass spectra were recorded by an Advion ExpressionL Compact Mass Spectrometer (CMS) (Ithaca, NY, USA) coupled with a KD Scientific Legato® 100 syringe pump at a flow rate of 10 µL/min. Samples were prepared at 0.1 mg/mL in methanol.

Matrix Assisted Laser Desorption/Ionization-Time of Flight Mass Spectrometry (MALDI-ToF) spectra were conducted using trans-2-[3-(4-tbutylphenyl)-2-methyl-2-propenylidene]malononitrile (DCTB) as matrix on a rapifleXTM MALDI-ToF/ToF mass spectrometer from Bruker with a 10 kHz scanning smartbeam threedimensional laser (Nd:YAG at 355 nm) and a 10-bit 5 GHz digitizer in positive ion reflector mode. Data were evaluated with mMass version 5.5.0 and plotted with GraphPad PRISM version 5.02.

Dynamic Light Scattering

Conventional Single Angle Dynamic Light Scattering

Dynamic light scattering (DLS) measurements were performed on a Zetasizer Nano ZS (Malvern Instruments Ltd, Malvern, U.K.) equipped with a HeNe laser (λ = 633 nm) and detected at a scattering angle of 173° at 25 °C. Dust was removed from the sample prior to each measurement by filtration through hydrophilic PTFE syringe filter (0.45 µm pore size, Acrodisc). The obtained data were processed by cumulant fitting for Z-average and PDI as well as by CONTIN fitting for particle size distribution. Visualization of the data were performed using GraphPad Prism version 5.02.

Multi Angle Dynamic Light Scattering

For multi angle dynamic light scattering (DLS) measurements of plasma incubated polymer micelles, the samples were filtered through LCR membrane syringe filters (0.45 µm pore size, PALL Life Science). Citrate-stabilized human plasma was filtered through GS membrane syringe filters (0.2 µm pore size, PALL Life Science). The samples were mixed in a volume ratio of 80% plasma and 20% micellar PBS solution in dust-free scattering cuvettes and incubated at 37 °C for 1 h. Subsequent DLS measurements were performed with a Uniphase He/Ne Laser (632.8 nm, 22 mW), an ALV-SP125 Goniometer, an ALV/High QE APD-Avalanche photodiode, an ALV5000/E/PCI-correlator and a Lauda RC-6 thermostat unit. The angular dependent measurements were performed between 30° and 150° in 30° steps. Data analysis was performed according to the procedure described by Rausch and co-workers.[1] Visualization of the data were performed using OriginPro 2021b version 9.8.5.212 from OriginLab Corporation.

Ultraviolet-Visible Spectroscopy

UV-vis spectra were measured using a Thermo Scientific™ NanoDrop™ 2000c spectrophotometer. A Spark 20M Multimode Microplate Reader from TecanTrading AG (Mannedorf, Switzerland) was utilized for QUANTI-Blue™ and MTT assays.

Electron Microscopy

Transmission electron microscopy (TEM) samples were prepared in TRIS buffer (0.05 M, pH = 7.4) at a polymer mass concentration of β = 2 mg/mL. The analysis was performed on a Tecnai T12 or a Tecnai

G2 Spirit from FEI (Hillsboro, USA), both equipped with a LaB_6 cathode operating at 120 kV. The former is equipped with a BioTWIN objective lens whereas the latter makes use of a TWIN lens. Images were recorded either using a MegasSYS 1k×1k or a Gatan US1000 2k×2k CCD sensor. 5 µL of the sample were left to absorb to freshly glow discharged copper grids (CF300-Cu, 300 mesh) coated with a 3–4 nm carbon film from Electron Microscopy Sciences (Hatfield, USA) for 1 min and negatively stained afterwards for 20 s with 5 µL of a 2 wt% solution of uranyl acetate. Excess liquid was removed with Whatman® grade 1 filter papers from GE Healthcare Biosciences (Uppsalla, Sweden) after each step.

MONOMER SYNTHESIS

2,2-dibenzyloxypropane (BisBnKetal, 3)

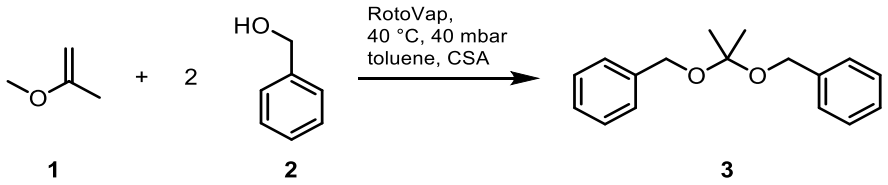

1 **2** **3**

A round bottom flask (RBF) was charged with 200 mL toluene, 2-methoxypropene (**1**) (10.0 mL, 104 mmol, 1.00 eq) and benzyl alcohol (**2**) (32.5 mL, 313 mmol, 3.00 eq). To this solution camphorsulfonic acid (CSA, 0.243 g, 1.04 mmol, 0.01 eq) was added and the mixture was stirred at room temperature for 2 h. The addition of one equivalent benzyl alcohol **2** to 2-methoxypropene (**1**) was confirmed by thin layer chromatography (TLC), before the reaction was continued at the rotary evaporator (40 mbar, 40 °C) for 4 h. Subsequently, the reaction was quenched with trimethylamine (TEA, 1.05 g, 1.45 mL, 0.1 eq.). The residual solvent was evaporated under reduced pressure and the crude product was purified by silica column chromatography (CH:EA = 10:1, 0.05vol% TEA), yielding bis-BnKetal (**3**) (25.10 g, 97.90 mmol, 94%) as a colorless oil.

^{1}H NMR (300 MHz, DMSO-d_6) δ [ppm]: 7.37–7.32 (m, 10H, Ar-*H*); 4.52 (s, 4H, Ar-CH_2-), 1.45 (s, 6H, CH_3-).

^{13}C NMR (75 MHz, DMSO-d_6) δ [ppm]: 138.9; 128.2; 127.3; 127.1; 100.3; 62.5; 25.0.

ESI-MS: m/z = 279.17 $[M+Na]^+$.

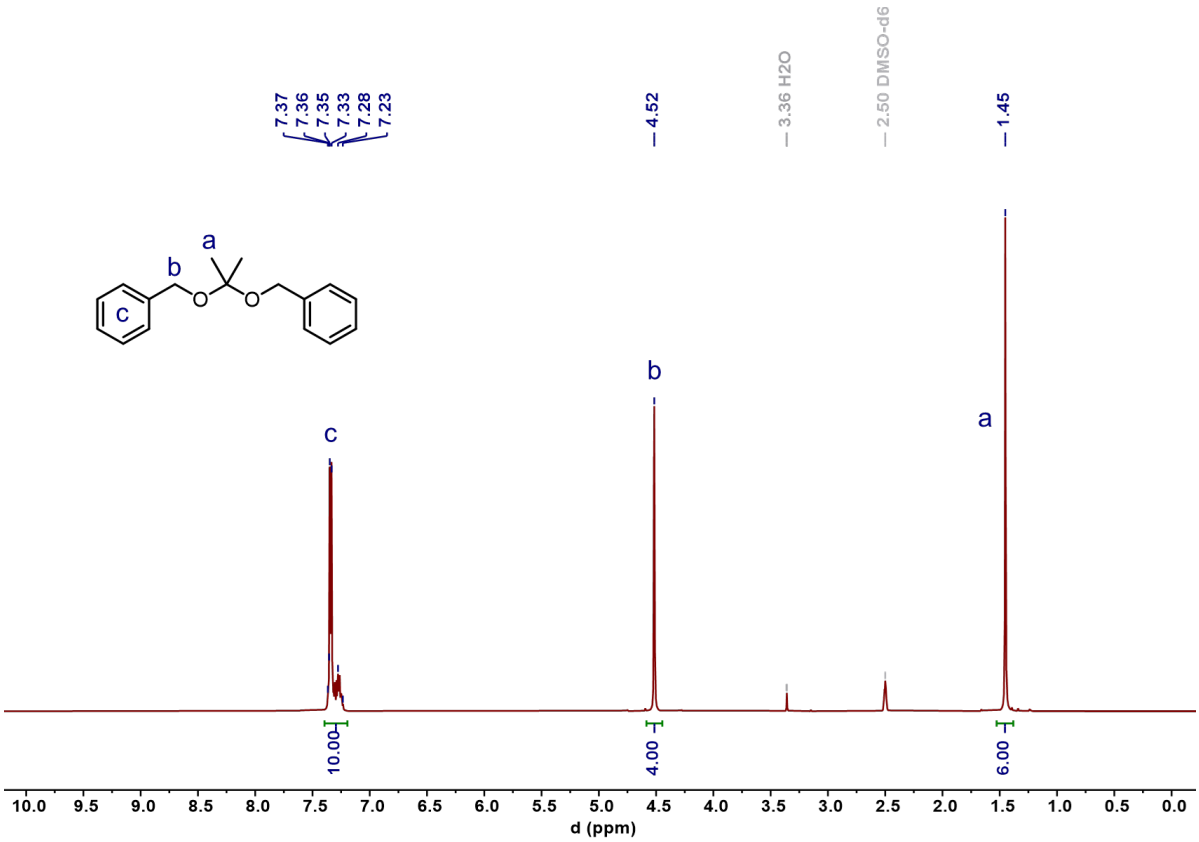

Figure S1: ^{1}H NMR spectrum (300 MHz, DMSO-d_6) of 2,2-dibenzyloxypropane (BisBnKetal, **3**).

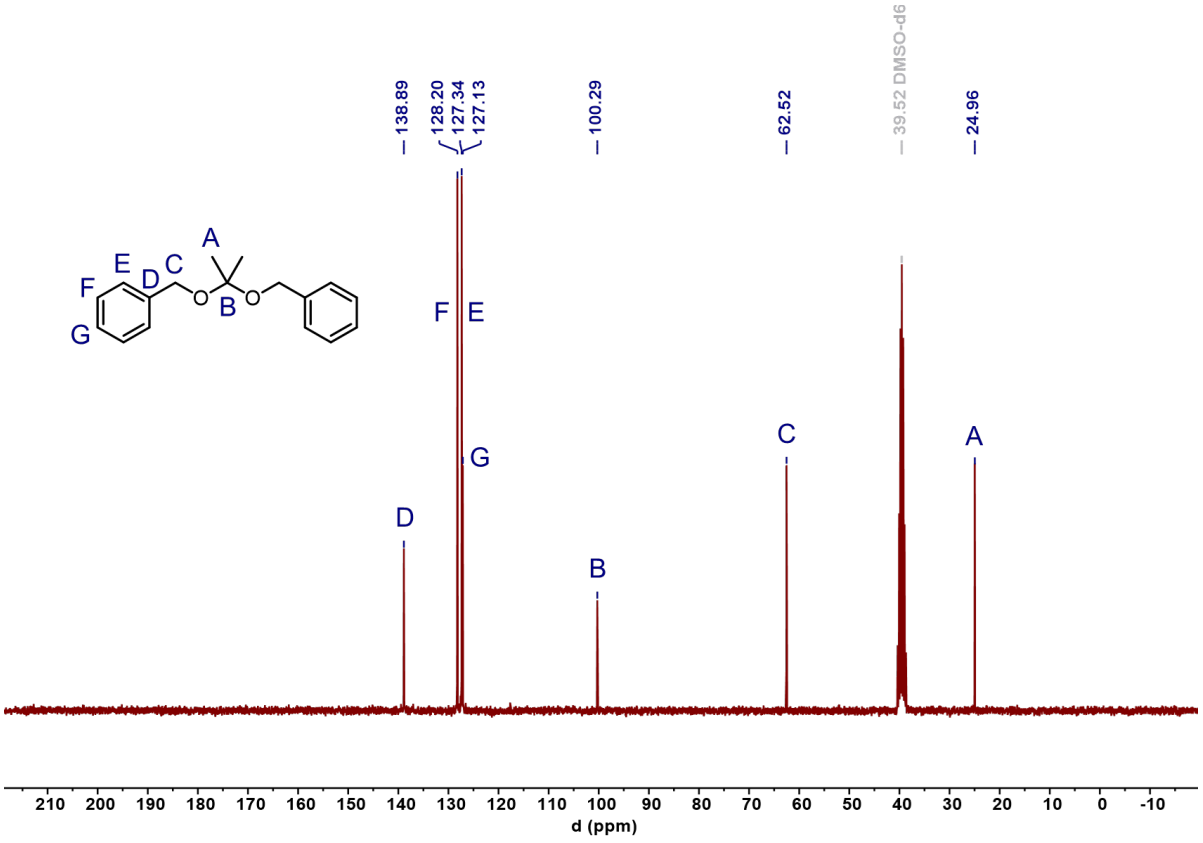

Figure S2: ^{13}C NMR spectrum (75 MHz, DMSO-d_6) of 2,2-dibenzyloxypropane (BisBnKetal, **3**).

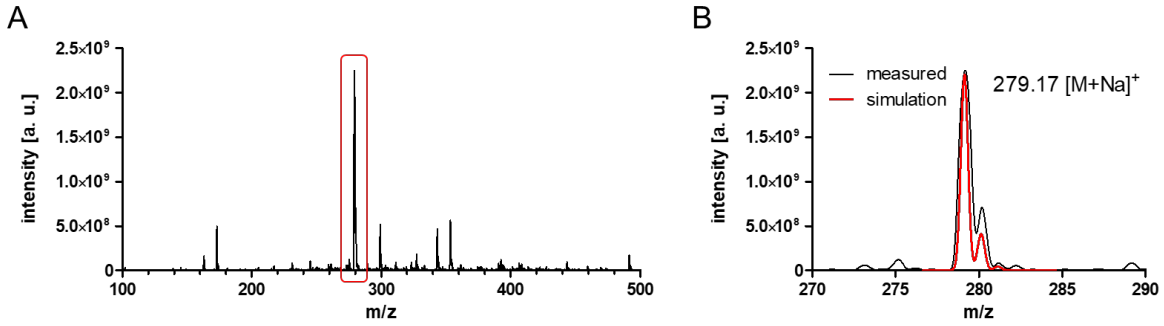

Figure S3: ESI-MS of 2,2-dibenzyloxypropane (BisBnKetal, **3**). **A**: Full spectrum with red box marking the magnified are in **B**: Na^+ ionized peak with simulation in red.

Ethylene glycol monoacetate (EGMA, 6)

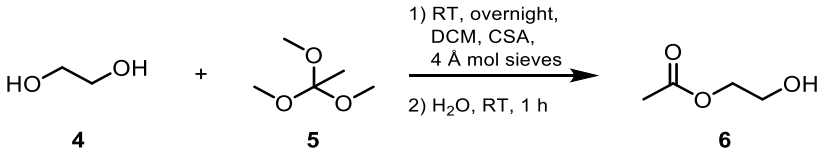

Ethylene glycol (**4**) (4.50 mL, 80.5 mmol, 1.00 eq) and trimethyl orthoacetate (**5**) (13.3 mL, 105 mmol, 1.30 eq) were dissolved in 85 mL dry DCM. To this solution 4 Å molecular sieves and CSA (0.37 g, 1.61 mmol, 0.02 eq) were added. After overnight stirring, water (2.18 mL, 121 mmol, 1.50 eq) was added and stirring was continued for 1 h. The solvent was evaporated under reduced pressure and the residue was purified by silica column chromatography (100% EA) yielding EGMA (**6**) (7.60 g, 73.0 mmol, 91%) as a colorless oil.

^{1}H NMR (300 MHz, $CDCl_3$) δ [ppm]: 4.08–4.05 (m, 2H, AcO-C*H*$_2$-); 3.71–3.66 (m, 2H, HO-C*H*$_2$-); 3.23 (t, J = 6.00 Hz, 1H, -O*H*); 1.98 (s, 3H, -C*H*$_3$).

^{13}C NMR (75 MHz, $CDCl_3$) δ [ppm]: 171.6; 66.1; 61.0; 20.9.

ESI-MS: m/z = 105.09 $[M+H]^+$, 127.10 $[M+Na]^+$.

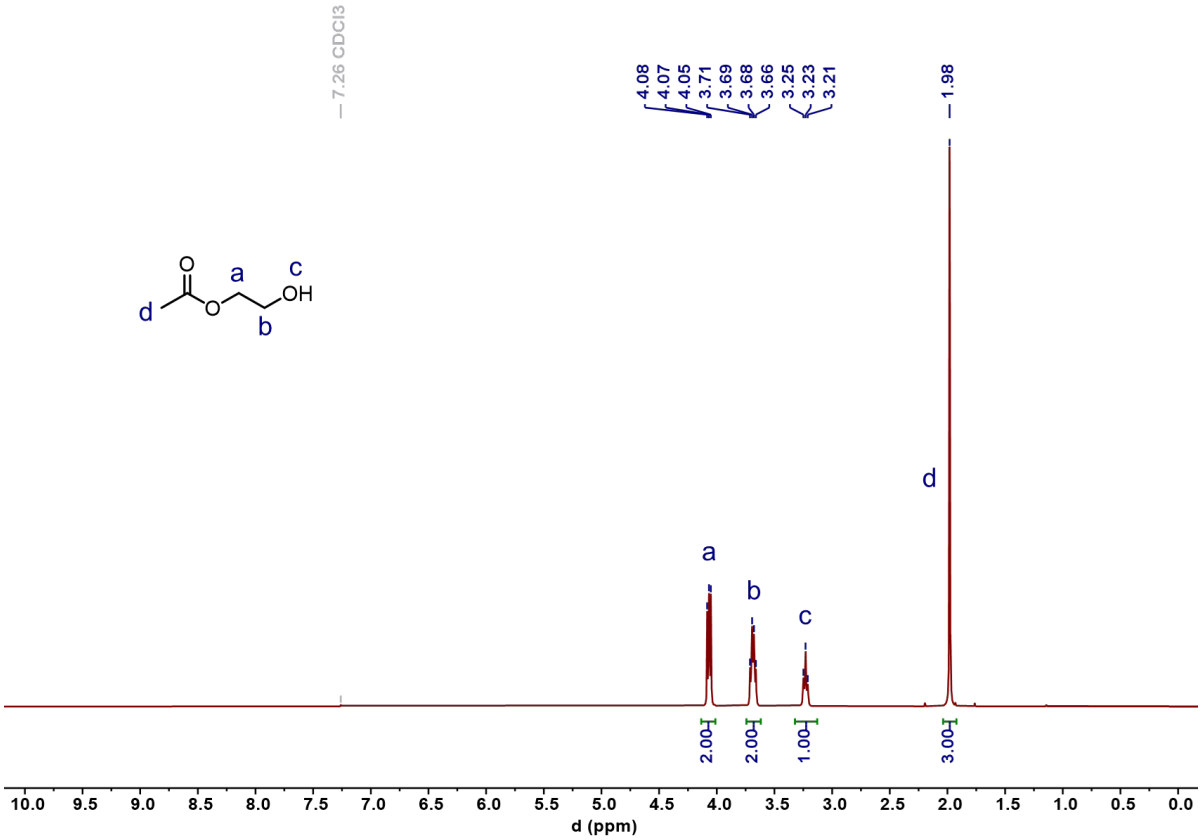

Figure S4: ^{1}H NMR spectrum (300 MHz, $CDCl_3$) of ethylene glycol monoacetate (EGMA, **6**).

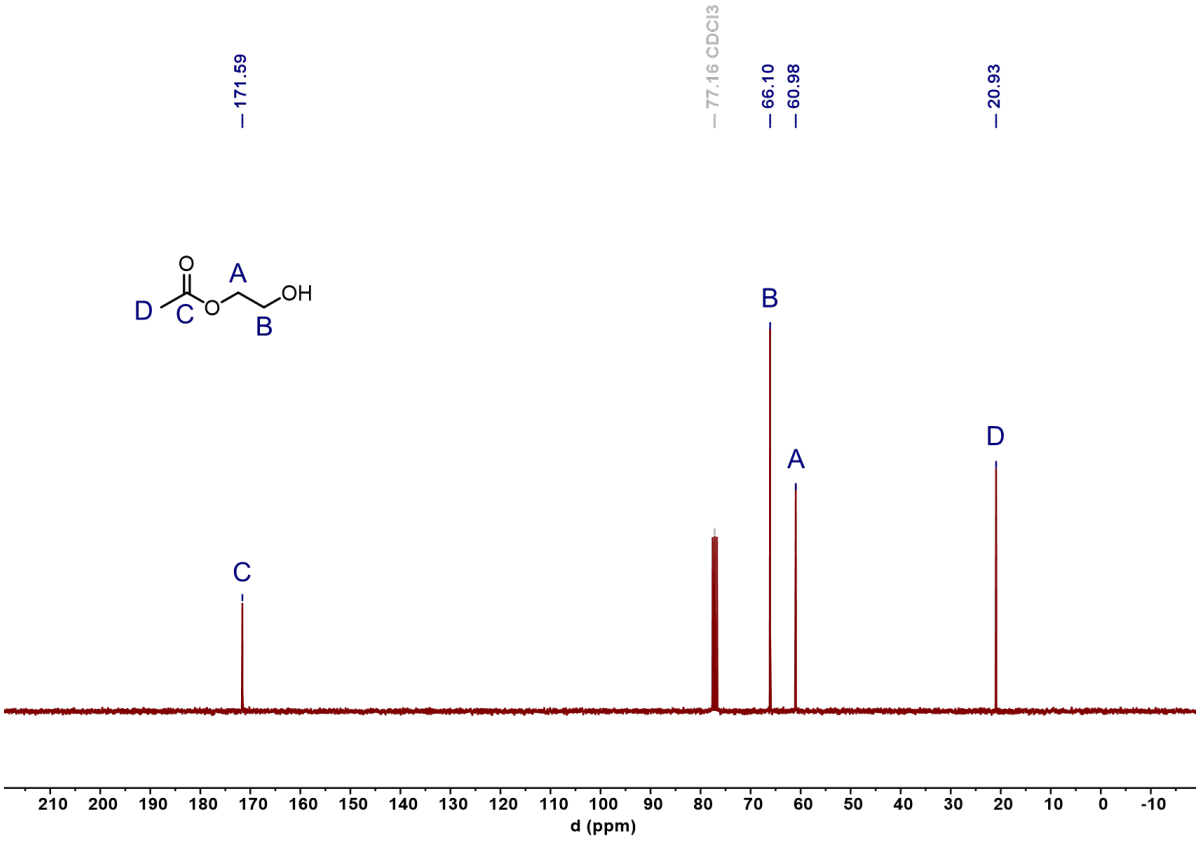

Figure S5: ^{13}C NMR spectrum (75 MHz, $CDCl_3$) of ethylene glycol monoacetate (EGMA, **6**).

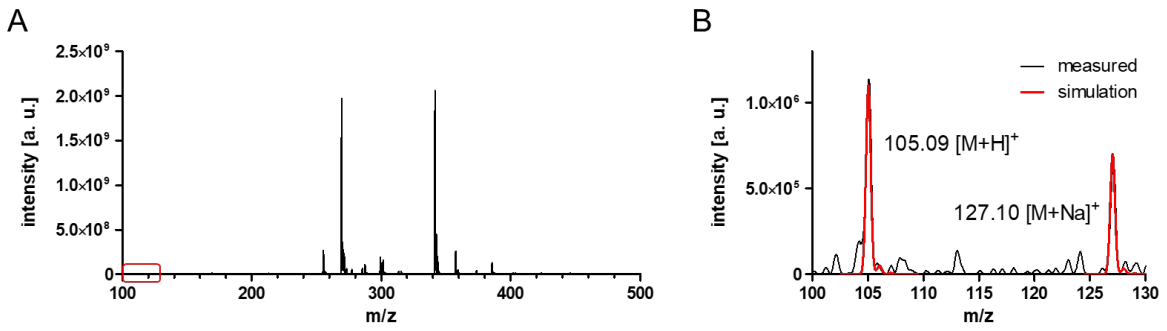

Figure S6: ESI-MS of ethylene glycol monoacetate (EGMA, **6**). **A**: Full spectrum with red box marking the magnified are in **B**: H^+ and Na^+ ionized peak with simulation in red.

2-acetoxyethoxy-2-benzyloxypropane 7

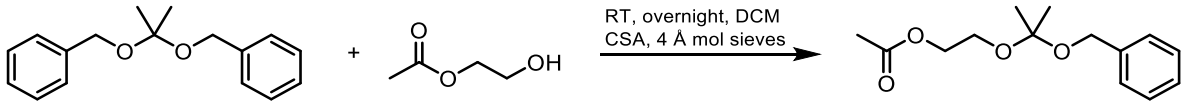

3 **6** **7**

In a RBF BisBnKetal **3** (3.50 g, 13.7 mmol, 1.00 eq) and EGMA (**6**) (4.26 g, 41.0 mmol, 3.00 eq) were dissolved in 50 mL dry THF. After the addition of 4 Å molecular sieves and CSA (31.7 mg, 0.14 mmol, 0.01 eq), the mixture was stirred overnight at room temperature. The reaction was quenched with TEA (0.19 mL, 1.37 mmol, 0.10 eq) and the solvent was evaporated under reduced pressure. The crude product was purified by silica column chromatography (CH:EA = 12:1, 0.05vol% TEA) leading to 2-acetoxyethoxy-2-benzyloxypropane (**7**) (1.60 g, 6.34 mmol, 46%) as colorless oil.

^{1}H NMR (300 MHz, DMSO-d_6) δ [ppm]: 7.34–7.26 (m, 5H, Ar-*H*); 4.46 (s, 2H, Ar-C*H*$_2$-); 4.13–4.10 (m, 2H, AcO-C*H*$_2$-); 3.63–3.60 (m, 2H, AcO-CH$_2$-C*H*$_2$-O-); 1.94 (s, 3H, C*H*$_3$-(C=O)-O-); 1.36 (s, 6H, C*H*$_3$-C-).

^{13}C NMR (75 MHz, DMSO-d_6) δ [ppm]: 170.3; 138.9; 128.2; 127.3; 127.1; 99.9; 63.4; 62.2; 58.7; 24.8; 20.6.

ESI-MS: m/z = 275.37 $[M+Na]^+$.

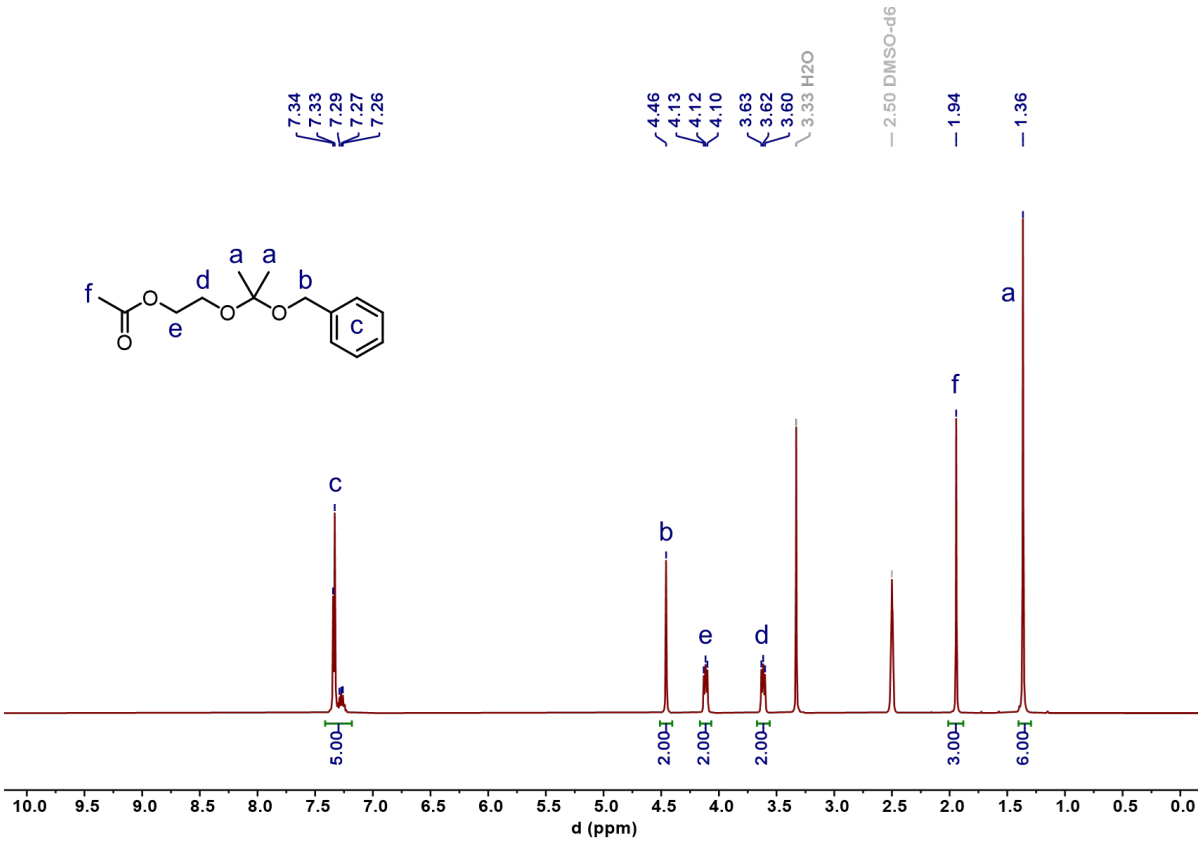

Figure S7: ^{1}H NMR spectrum (300 MHz, DMSO-d_6) of 2-acetoxyethoxy-2-benzyloxypropane (**7**).

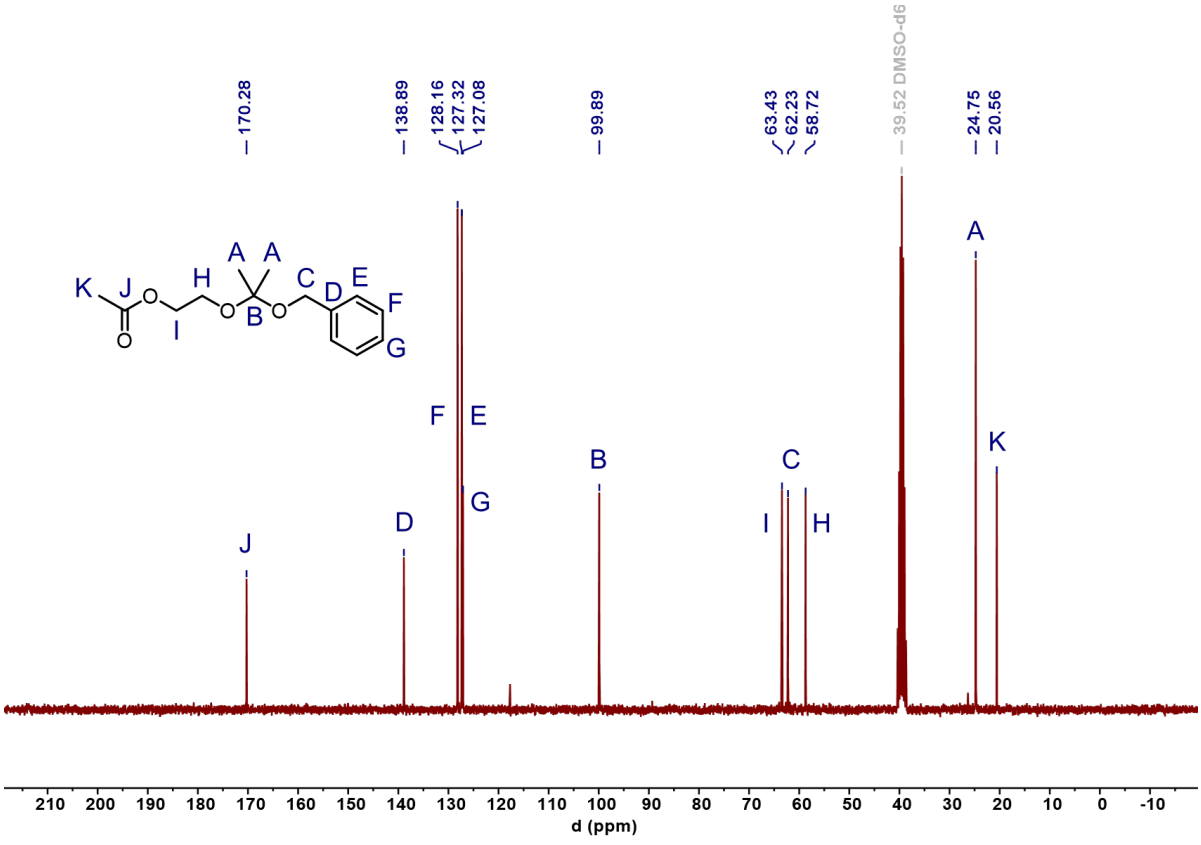

Figure S8: ^{13}C NMR spectrum (75 MHz, DMSO-d_6) of 2-acetoxyethoxy-2-benzyloxypropane (**7**).

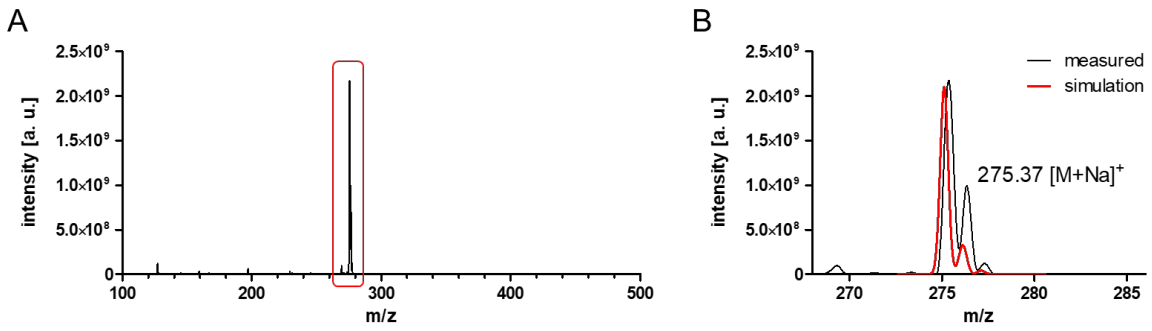

Figure S9: ESI-MS of 2-acetoxyethoxy-2-benzyloxypropane (**7**). **A**: Full spectrum with red box marking the magnified are in **B**: Na^+ ionized peak with simulation in red.

2-hydroxyethoxy-2-benzyloxypropane (8)

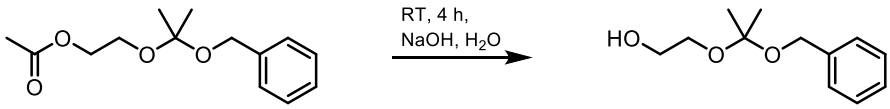

7 **8**

A RBF was charged with NaOH (1.01 g, 25.4 mmol, 4.00 eq) and 40 mL DI water. After complete solution of NaOH, 2-acetoxyethoxy-2-benzyloxypropane (**7**) (1.60 g, 6.34 mmol, 1.00 eq) was added. The two-phase mixture was stirred at room temperature for 4 h. After confirming full conversion via TLC, the aqueous solution was extracted with DCM, to which 0.5vol% DIPEA were added (3 x 50 mL). The combined organic layers were dried over Na_2SO_4 and concentrated under reduced pressure, leading to 2-hydroxyethoxy-2-benzyloxypropane (**8**) (1.27 g, 6.04 mmol, 95%) as a colorless oil.

^{1}H NMR (300 MHz, DMSO-d_6) δ[ppm]: 7.34–7.26 (m, 5H, Ar-*H*); 4.62 (t, J = 4.50 Hz 1H, -O*H*); 4.45 (s, 2H, Ar-CH_2-); 3.54–3.41 (m, 4H, HO-CH_2-CH_2-); 1.35 (s, 6H, CH_3-C-).

^{13}C NMR (75 MHz, DMSO-d_6) δ[ppm]: 139.1; 128.1; 127.5; 127.1; 99.6; 62.4; 62.2; 60.4; 24.9.

ESI-MS: m/z = 233.29 $[M+Na]^+$.

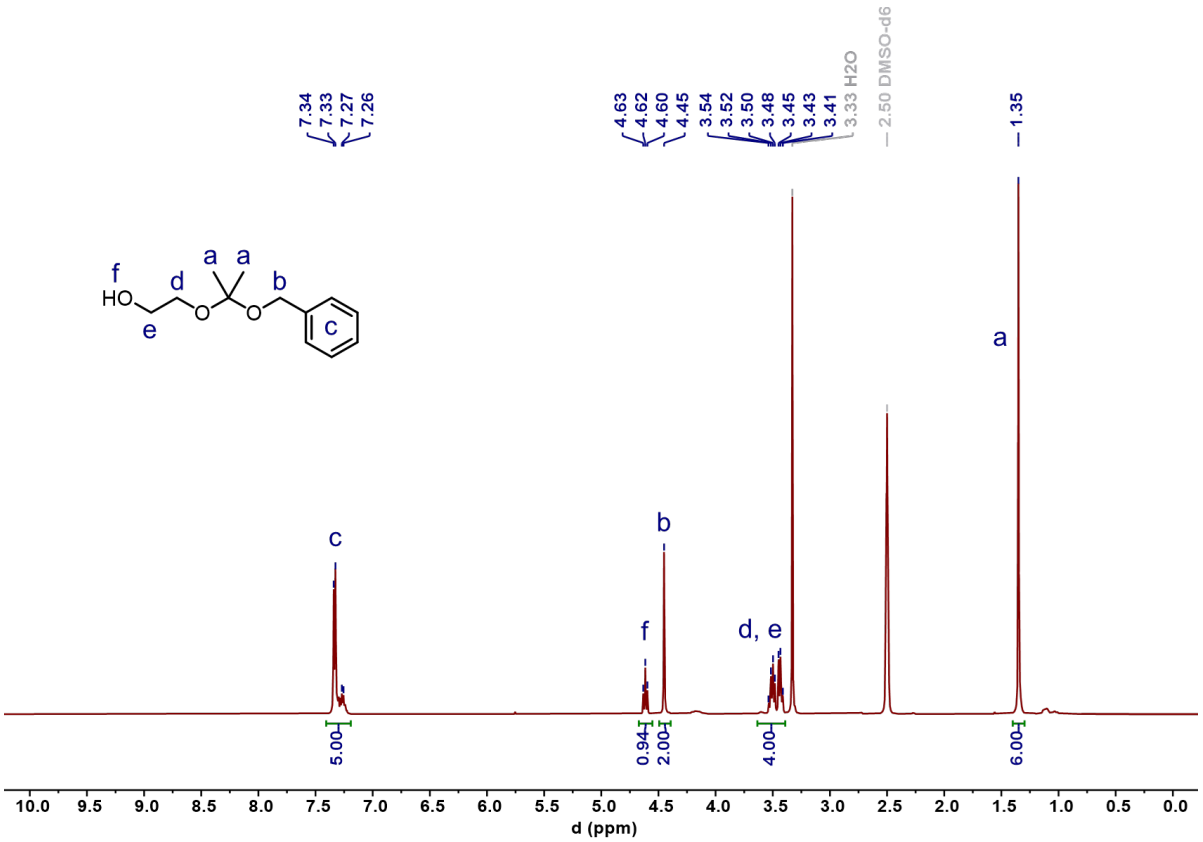

Figure S10: ^{1}H NMR spectrum (300 MHz, DMSO-d_6) of 2-hydroxyethoxy-2-benzyloxypropane (**8**).

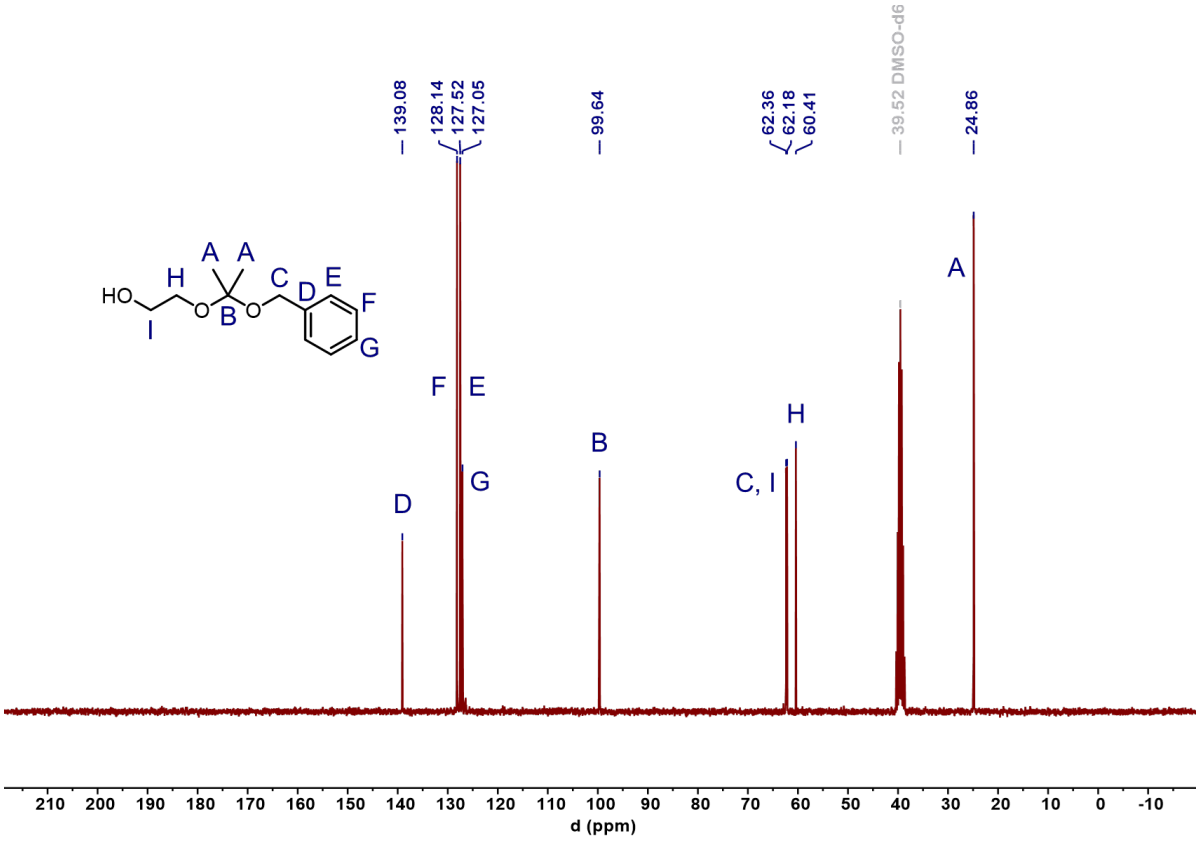

Figure S11: ^{13}C NMR spectrum (75 MHz, DMSO-d6) of 2-hydroxyethoxy-2-benzyloxypropane (**8**).

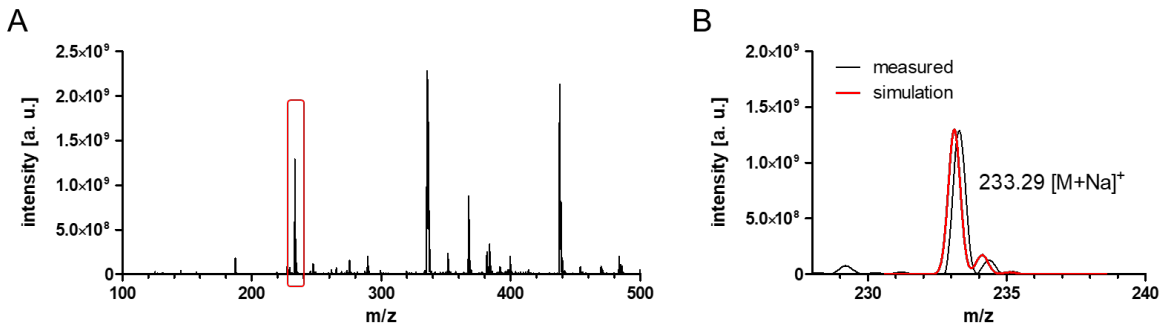

Figure S12: ESI-MS of 2-hydroxyethoxy-2-benzyloxypropane (**8**). **A**: Full spectrum with red box marking the magnified are in **B**: Na^+ ionized peak with simulation in red.

Benzyl-2,2-bis(hydroxymethyl)propionate (bis-MPABn, 11)

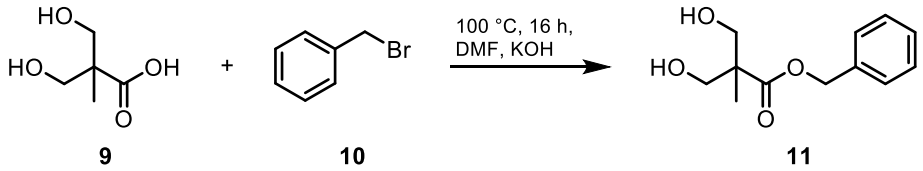

9 **10** **11**

Based on the literature,[2] 2,2-bis(hydroxymethyl)propionic acid (bis-MPA, **9**) (45.00 g, 336 mmol, 1.00 eq) and KOH (21.50 g, 338 mmol, 1.01 eq) were dissolved in 250 mL *N*,*N*-dimethylformamide (DMF). The mixture was heated to 100 °C for 1 h. To the hot solution benzyl bromide (**10**) (48.0 mL, 404 mmol, 1.20 eq) was added and stirring at 100 °C was continued for 16 h. After cooling, the solvent was evaporated under reduced pressure. 300 mL ethyl acetate, 300 mL hexane and 200 mL water were added. The organic layer was washed with further 200 mL DI water and dried over $MgSO_4$. Evaporation of the solvent led to a solid, that was recrystallized from toluene, yielding bis-MPABn (**11**) (45.03 g, 0.201 mmol, 60%) as white crystals.

^{1}H NMR (300 MHz, $CDCl_3$) δ [ppm]: 7.39–7.31 (m, 5H. Ar-*H*); 5.22 (s, 2H, Ar-C*H*$_2$-); 3.98–3.71 (m, 4H, HO-C*H*$_2$-); 2.76 (t, J = 7.50 Hz, 2H, -O*H*); 1.08 (s, 3H, -C*H*$_3$).

^{13}C NMR (75 MHz, $CDCl_3$) δ [ppm]: 175.7; 135.8; 128.7; 128.3; 127.9; 67.4; 66.7; 49.4; 17.2.

ESI-MS: m/z =247.09 $[M+Na]^+$.

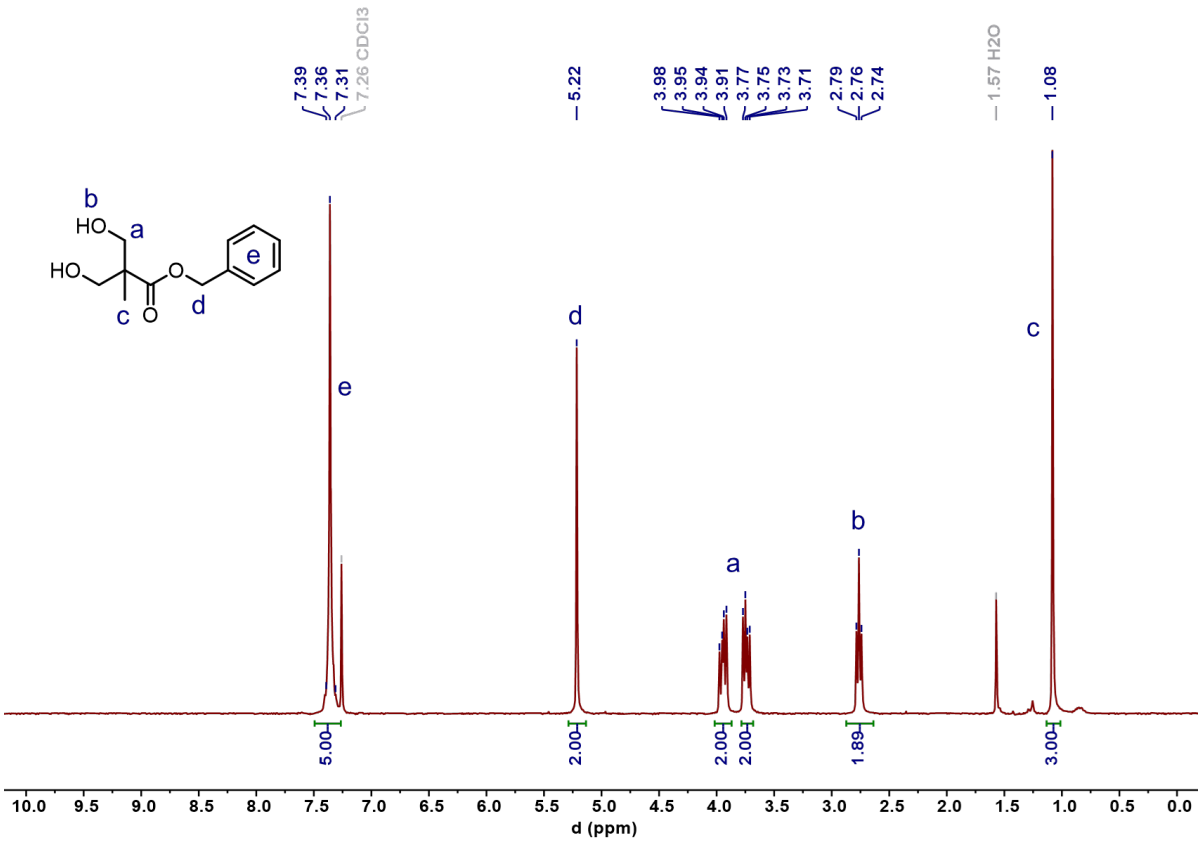

Figure S13: ^{1}H NMR spectrum (300 MHz, $CDCl_3$) of benzyl-2,2-bis(hydroxymethyl)propionate (bis-MPABn, **11**).

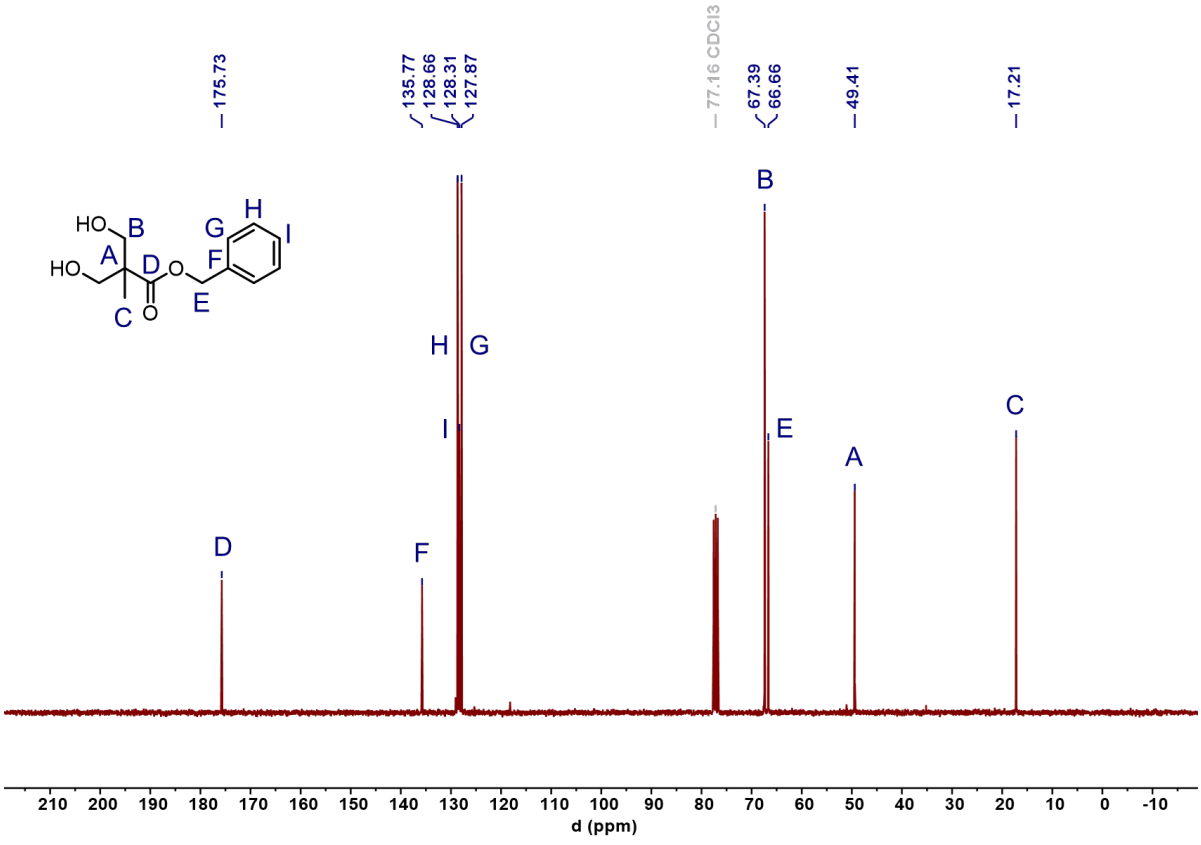

Figure S14: ^{13}C NMR spectrum (75 MHz, $CDCl_3$) of benzyl-2,2-bis(hydroxymethyl)propionate (bis-MPABn, **11**).

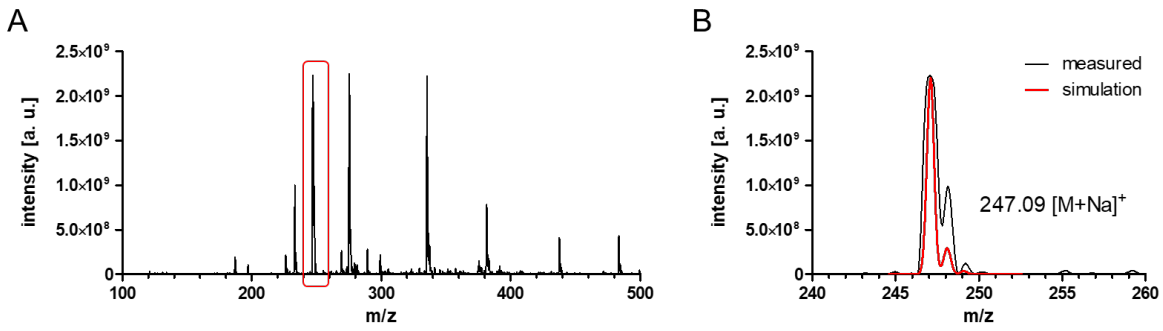

Figure S15: ESI-MS of benzyl-2,2-bis(hydroxymethyl)propionate (bis-MPABn, **11**). **A**: Full spectrum with red box marking the magnified are in **B**: Na^+ ionized peak with simulation in red.

5-methyl-5-benzyloxycarbonyl-1,3-dioxan-2-one (MTC-OBn, 12)

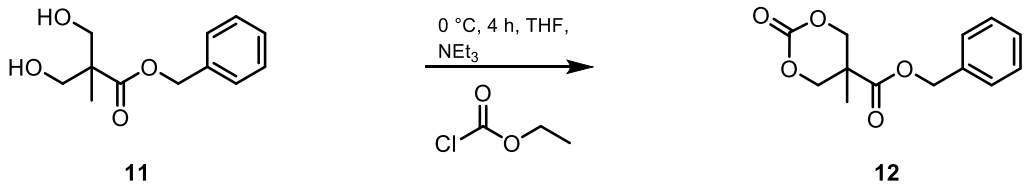

Based on the literature,[2,3] benzyl-2,2-bis(hydroxymethyl)propionate (**11**) (22.43 g, 100 mmol, 1.00 eq) was dissolved in 1.5 L THF. Ethyl chloroformate (56.0 mL, 588 mmol, 5.88 eq) was added and the mixture was cooled to 0 °C. Over a period of 30 min, TEA (86.1 mL, 618 mmol, 6.18 eq) was added. The solution was allowed to warm to room temperature and stirred for 2 h. Precipitated triethylamine hydrochloride was filtered off. The filtrate was concentrated under reduced pressure. To the concentrated solution 56 mL THF and 56 mL Et_2O were added. The mixture was stored in the fridge for 16 h. Next day, the precipitated solid was filtered off and washed with Et_2O. The solid was recrystallized from THF and Et_2O (1:1) and dried under reduced pressure. MTC-OBn (**12**) (23.46 g, 93.75 mmol, 94%) was obtained as white crystals.

^{1}H NMR (300 MHz, $CDCl_3$) δ [ppm]: 7.42–7.31 (m, 5H, Ar-*H*); 5.22 (s, 2H, Ar-C*H*$_2$-); 4.71 (d, *J* = 12.0 Hz, 2H, O=C-O-C*H*$_2$-); 4.20 (d, *J* = 12.0 Hz, 2H, O=C-O-C*H*$_2$-); 1.34 (s, 3H, -C*H*$_3$).

^{13}C NMR (75 MHz, $CDCl_3$) δ [ppm]: 171.0; 147.5; 134.9; 128.8; 128.8; 128.3; 73.0; 68.0 40.3; 17.6.

ESI-MS: m/z = 289.23 $[M+K]^+$.

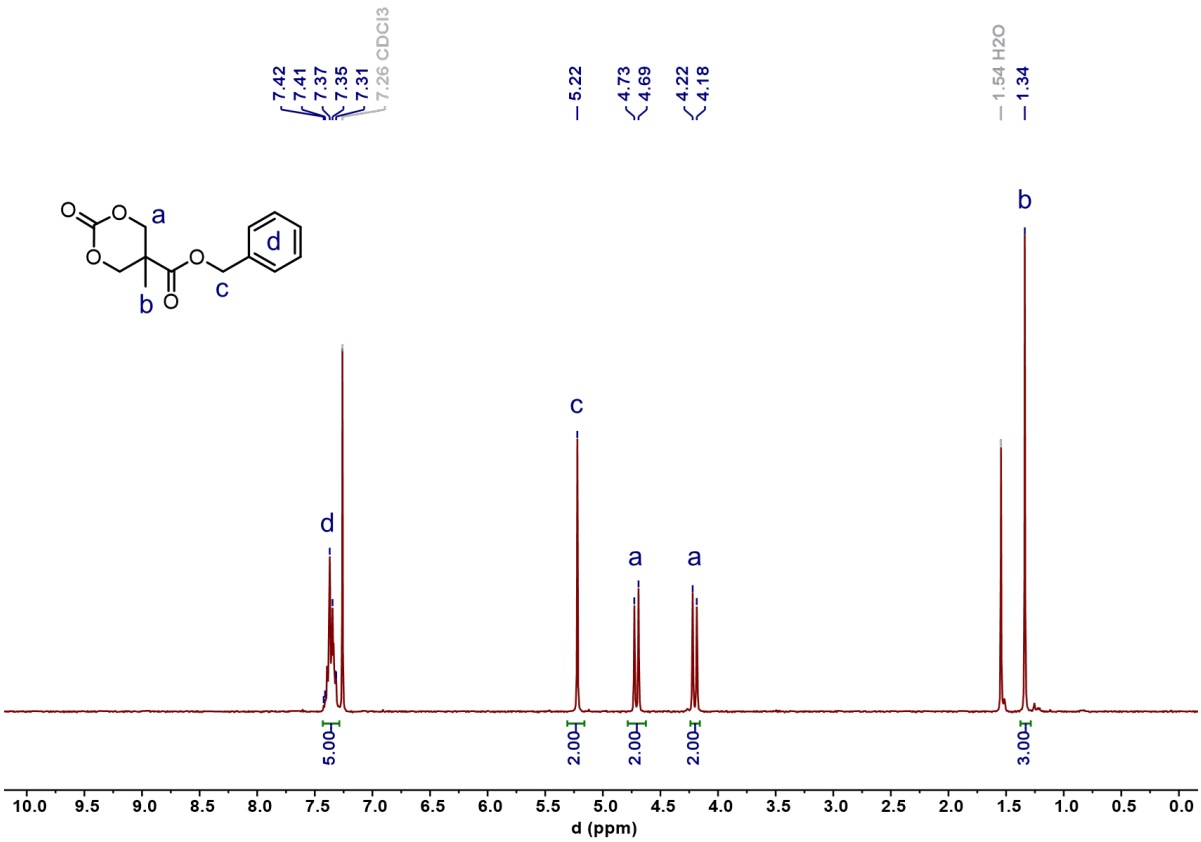

Figure S16: ^{1}H NMR spectrum (300 MHz, $CDCl_3$) of 5-methyl-5-benzyloxycarbonyl-1,3-dioxan-2-one (MTC-OBn, **12**).

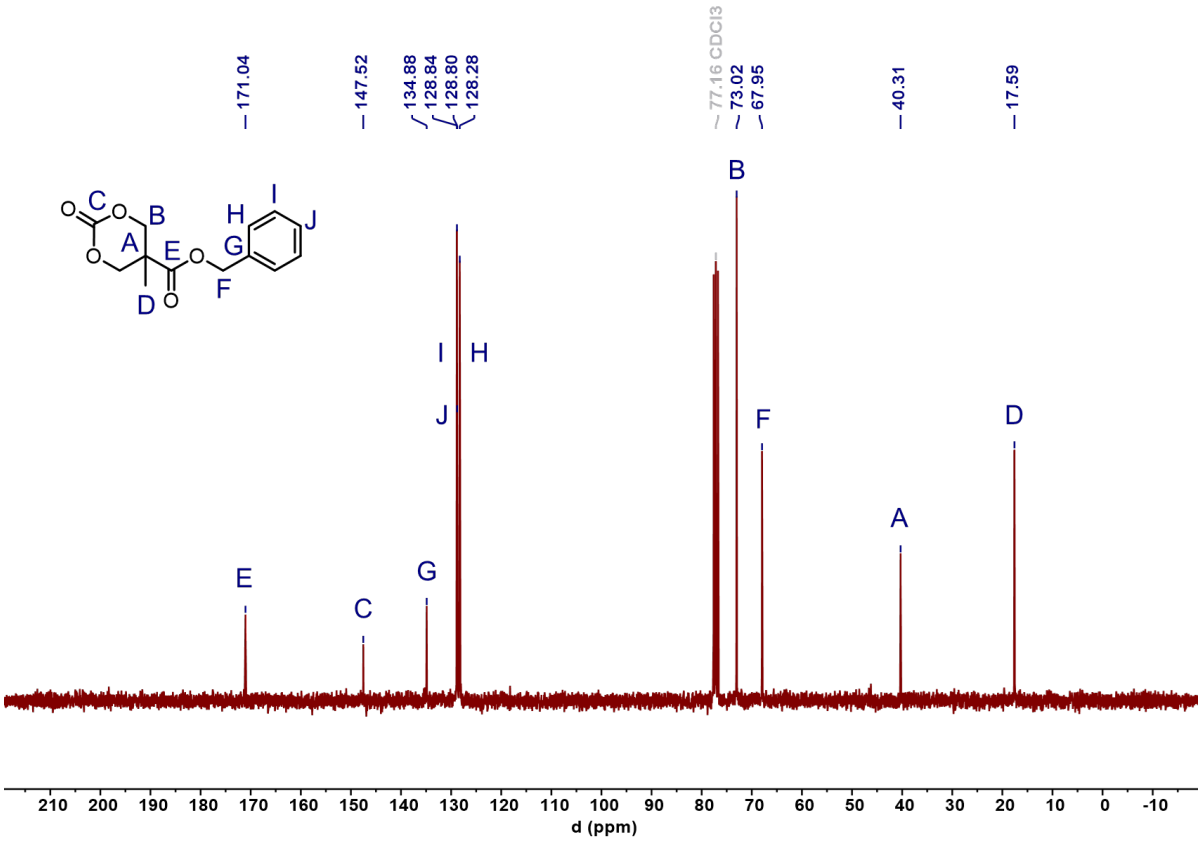

Figure S17: ^{13}C NMR spectrum (75 MHz, $CDCl_3$) of 5-methyl-5-benzyloxycarbonyl-1,3-dioxan-2-one (MTC-OBn, **12**).

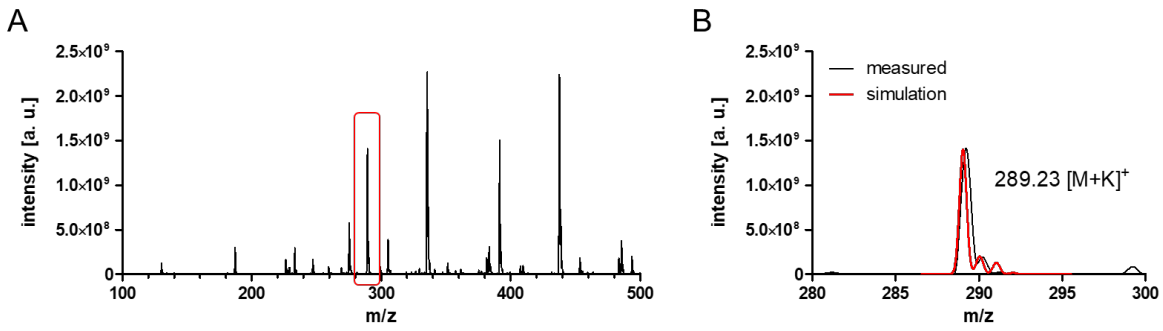

Figure S18: ESI-MS of 5-methyl-5-benzyloxycarbonyl-1,3-dioxan-2-one (MTC-OBn, **12**). **A**: Full spectrum with red box marking the magnified are in **B**: K^+ ionized peak with simulation in red.

5-methyl-1,3-dioxane-2-oxo-5-carboxylic acid (MTC-OH, 13)

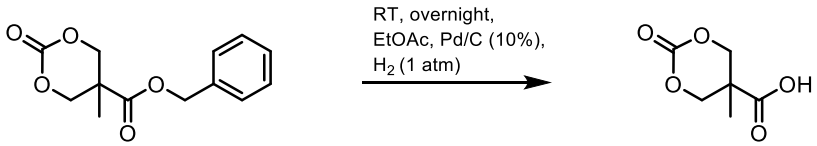

12 **13**

Based on the literature,[2] a RBF was charged with MTC-OBn (**12**) (25.03 g, 100 mmol, 1.00 eq) and 250 mL ethyl acetate. Pd/C (1.65 g, 10% w/w) was added, and the mixture was stirred overnight under H_2 atmosphere (1 atm). The suspension was mixed with 250 mL THF before being filtered through THF-wetted Celite®. The Celite® layer was washed with THF. The filtrate was concentrated under reduced pressure, leading to MTC-OH (**13**) (15.76 g, 98.42 mmol, 98%) as white crystals.

^{1}H NMR (300 MHz, DMSO-d_6) δ [ppm]: 13.43 (s, 1H, -COO*H*); 5.53 (d, J = 9.00 Hz, 2H, O=C-O-C*H*$_2$-); 4.31 (d, J = 9.00 Hz, 2H, O=C-O-C*H*$_2$-); 1.16 (s, 3H, -C*H*$_3$).

^{13}C NMR (75 MHz, DMSO-d_6) δ [ppm]: 171.0; 147.4; 72.8; 39.4; 16.5.

ESI-MS: m/z = 161.10 $[M+H]^+$, 183.01 $[M+Na]^+$.

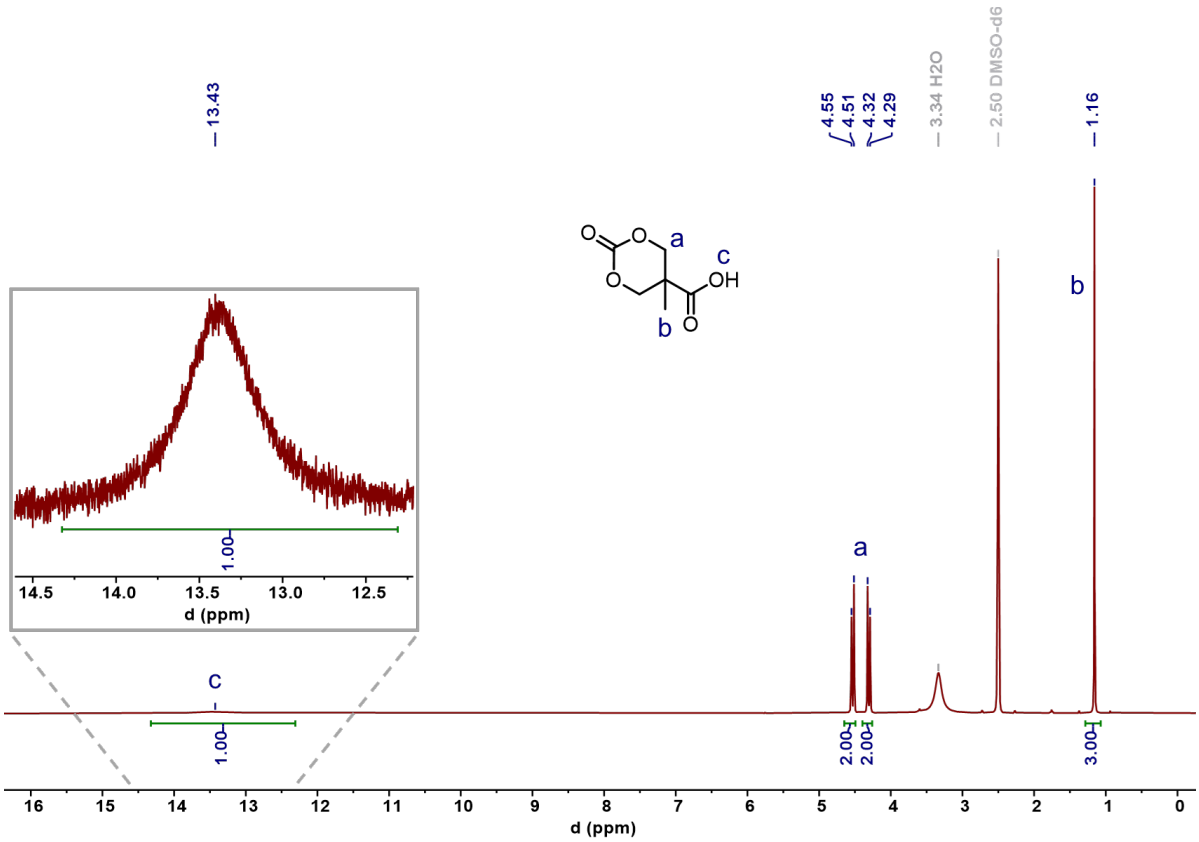

Figure S19: ^{1}H NMR spectrum (300 MHz, DMSO-d_6) of 5-methyl-1,3-dioxane-2-oxo-5-carboxylic acid (MTC-OH, **13**).

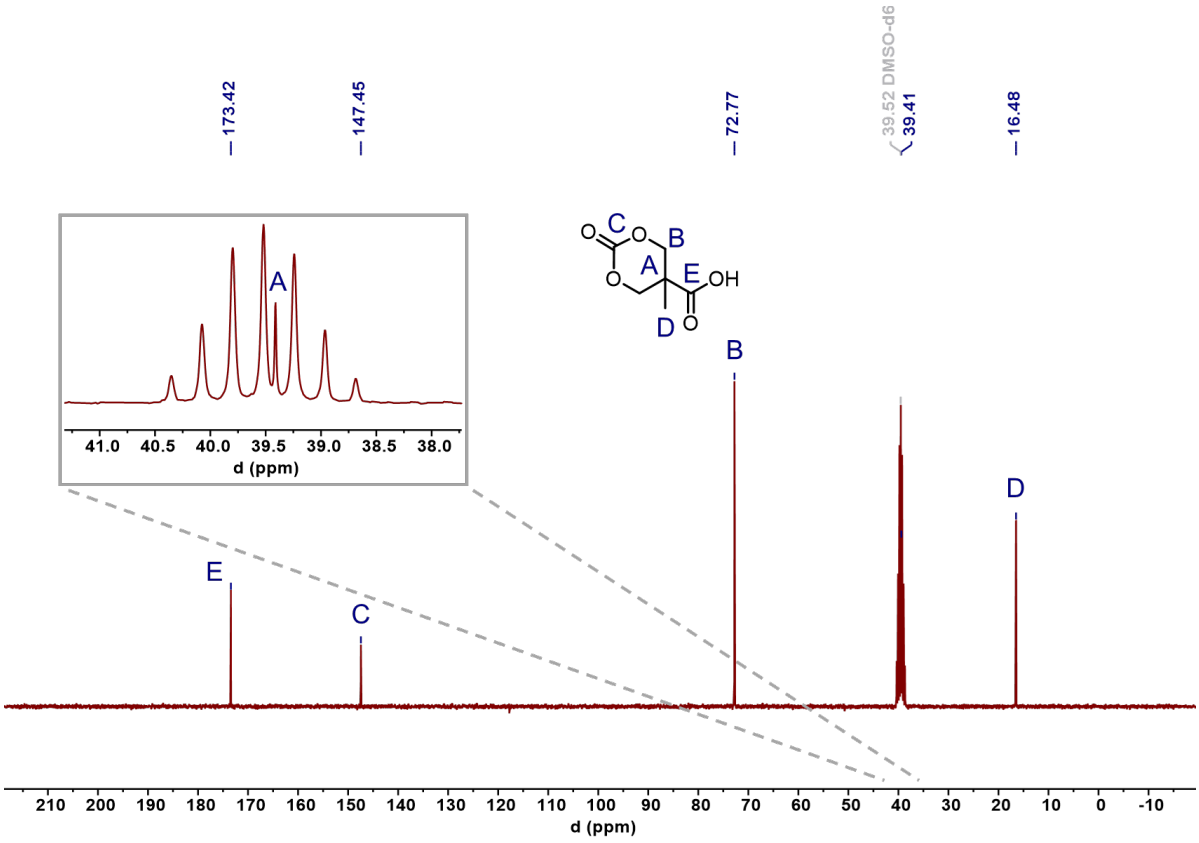

Figure S20: ^{13}C NMR spectrum (75 MHz, $CDCl_3$) of 5-methyl-1,3-dioxane-2-oxo-5-carboxylic acid (MTC-OH, **13**).

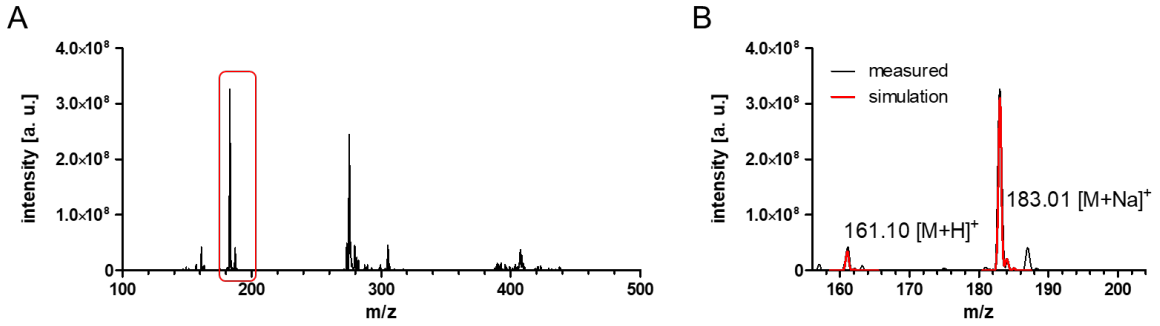

Figure S21: ESI-MS of 5-methyl-1,3-dioxane-2-oxo-5-carboxylic acid (MTC-OH, **13**). **A**: Full spectrum with red box marking the magnified are in **B**: H^+ and Na^+ ionized peak with simulation in red.

2-((2-(benzyloxy)propan-2-yl)oxy)ethyl 5-methyl-2-oxo-1,3-dioxane-5-carboxylate (MTC-OEtKBn, 14)

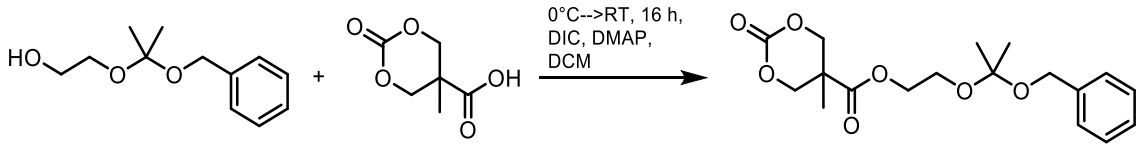

8 **13** **14**

A suspension of MTC-OH (**13**) (1.68 g, 10.5 mmol, 1.50 eq) and 4-dimethylaminopyridine (DMAP) (85.4 mg, 0.70 mmol, 0.10 eq) in 50 mL dry DCM was cooled to 0 °C. To the suspension, 2-hydroxyethoxy-2-benzyloxypropane (**8**) (1.47 g, 6.99 mmol, 1.00 eq) and *N,N'*-diisopropylcarbodiimide (DIC) (1.32 g, 10.5 mmol, 1.50 eq) were added. For a short time, a clear solution was formed, until 1,3-diisopropylurea started to precipitate. While overnight stirring, the solution was allowed to warm to room temperature. The white precipitate was filtered off, yielding an opaque liquid. The solvent was removed under reduced pressure and the residue was purified by silica column chromatography (CH:EA = 25:10, 0.05vol% TEA). MTC-OEtKBn (**14**) was obtained as colorless crystals (2.24 g, 6.36 mmol, 91%).

^{1}H NMR (300 MHz, DMSO-d$_6$) δ [ppm]: 7.35–7.26 (m, 5H, Ar-*H*); 4.50 (d, *J* = 12.0 Hz, 2H, O=C-O-C*H*$_2$-); 4.47 (s, 2H, Ar-C*H*$_2$-); 4.32 (d, *J* = 9.00 Hz, 2H, O=C-O-C*H*$_2$-); 4.29–4.26 (m, 2H, -(C=O)-O-C*H*$_2$-); 3.67–3.64 (m, 2H, -(C=O)-O-CH$_2$-C*H*$_2$-); 1.36 (s, 6H, -O-C-C*H*$_3$); 1.13 (s, 3H; -C=O-C-C*H*$_3$).

^{13}C NMR (75 MHz, DMSO-d$_6$) δ [ppm]: 171.6; 147.0; 138.9; 128.2; 127.2; 127.1; 100.0; 72.3; 64.8; 62.3; 58.5; 39.6; 24.7; 16.3.

ESI-MS: m/z = 375.14 $[M+Na]^+$, 391.07 $[M+K]^+$, 407.16 $[M+MeOH+Na]^+$, 423.09 $[M+MeOH+K]^+$.

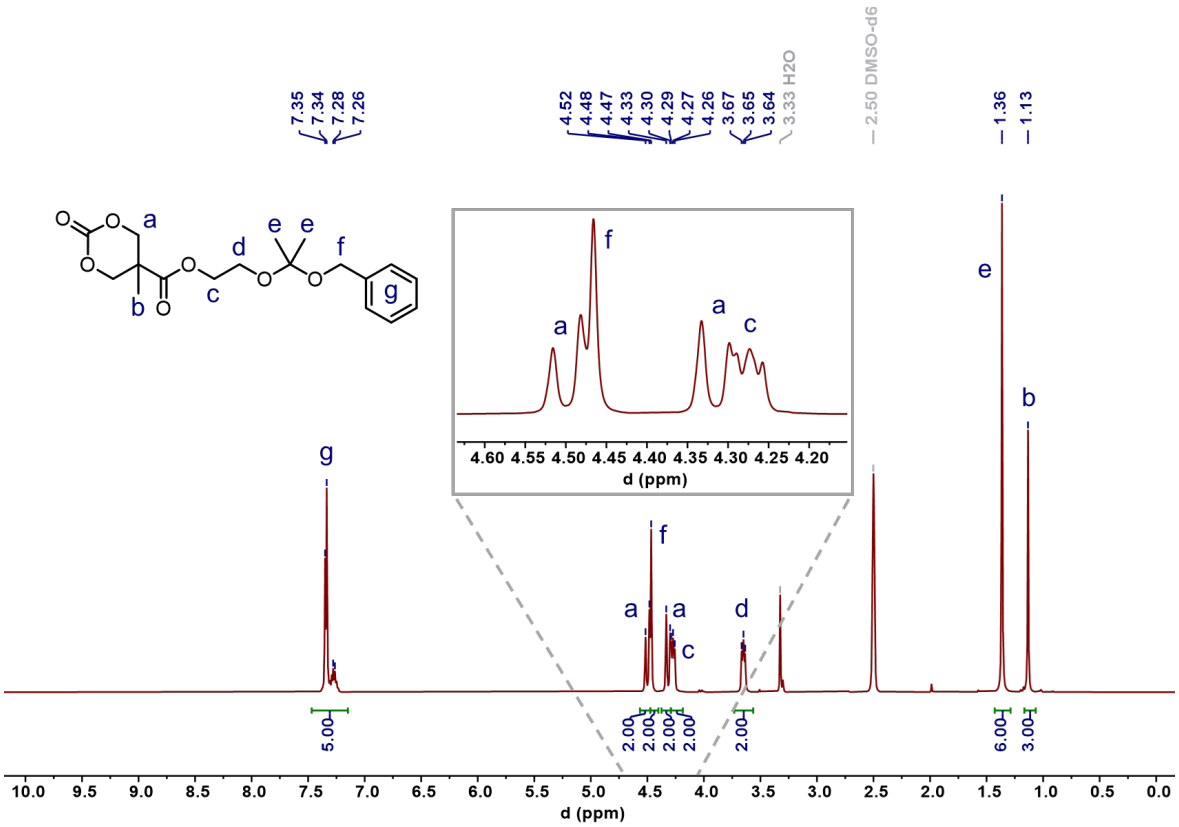

Figure S22: ^{1}H NMR spectrum (700 MHz, DMSO-d_6) of 2-((2-(benzyloxy)propan-2-yl)oxy)ethyl 5-methyl-2-oxo-1,3-dioxane-5-carboxylate (MTC-OEtKBn, **14**).

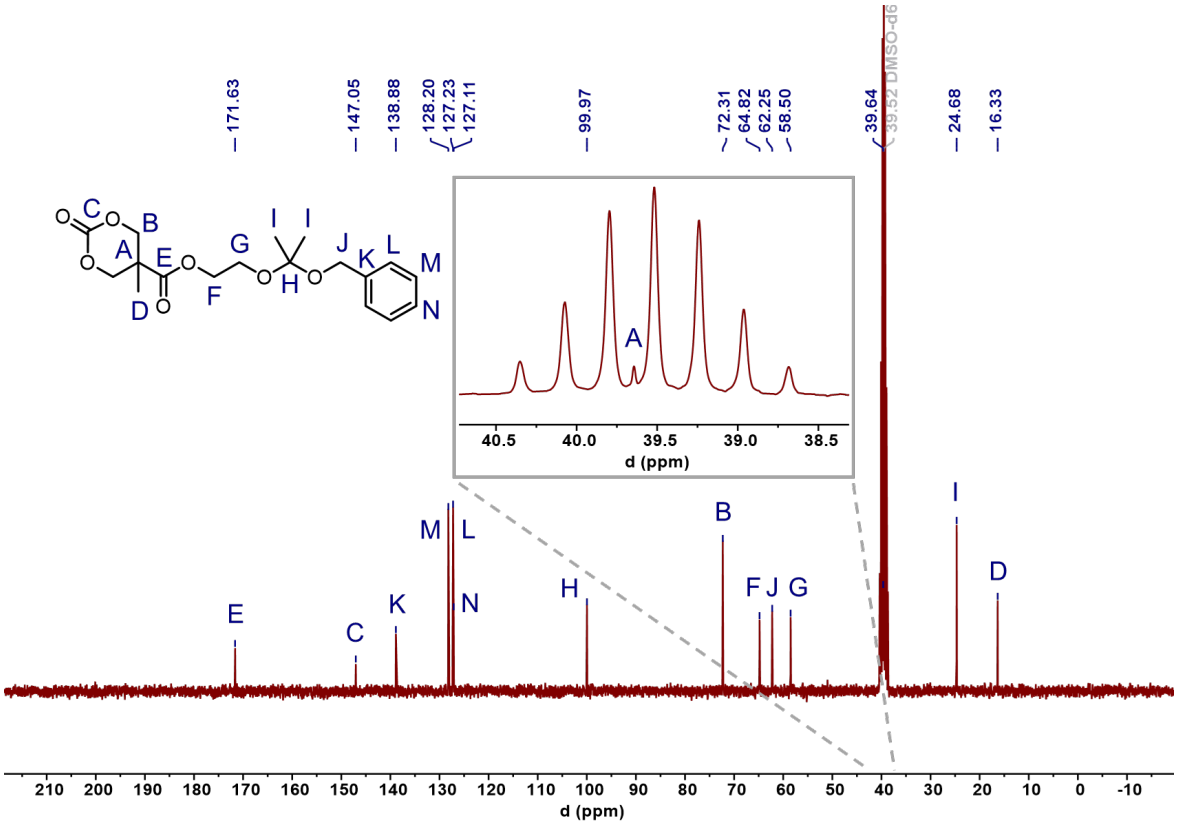

Figure S23: ^{13}C NMR spectrum (175 MHz, $CDCl_3$) of 2-((2-(benzyloxy)propan-2-yl)oxy)ethyl 5-methyl-2-oxo-1,3-dioxane-5-carboxylate (MTC-OEtKBn, **14**).

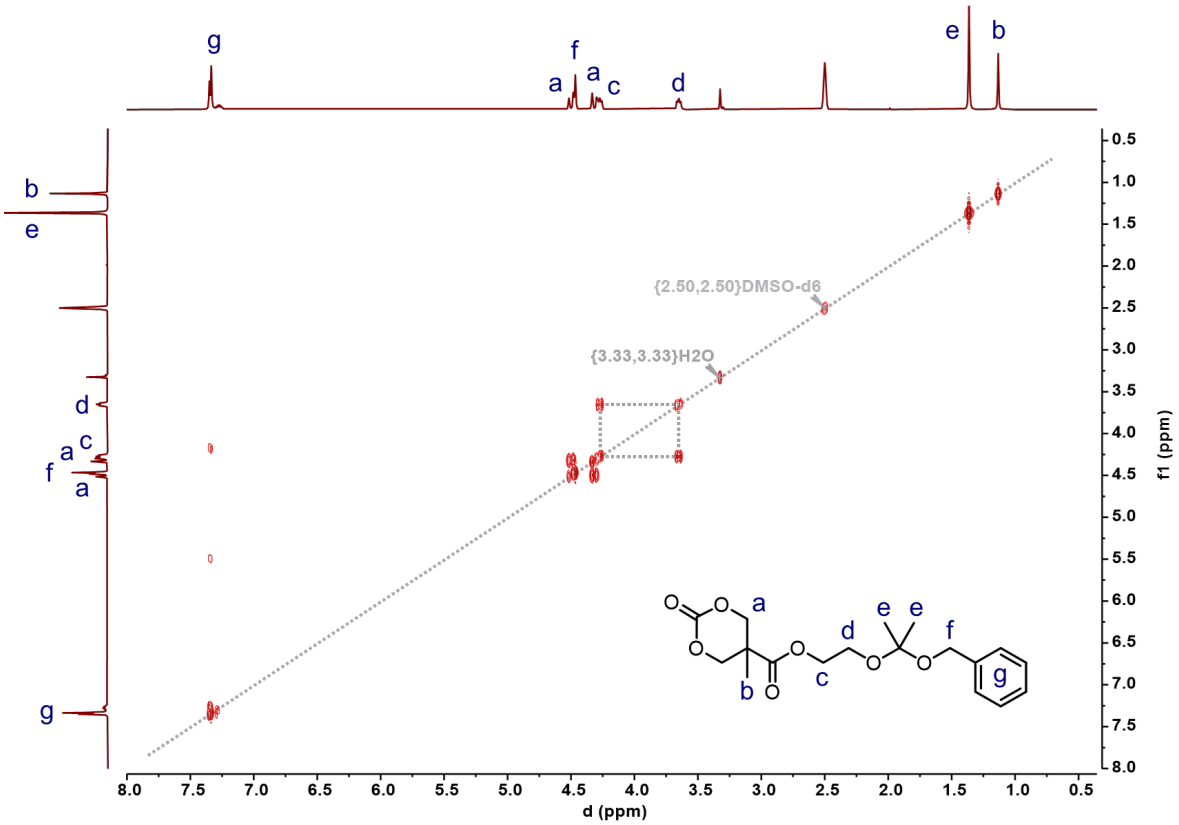

Figure S24: 2D ^{1}H,^{1}H-COSY spectrum (700 MHz, DMSO-d_6) of 2-((2-(benzyloxy)propan-2-yl)oxy)ethyl 5-methyl-2-oxo-1,3-dioxane-5-carboxylate (MTC-OEtKBn, **14**).

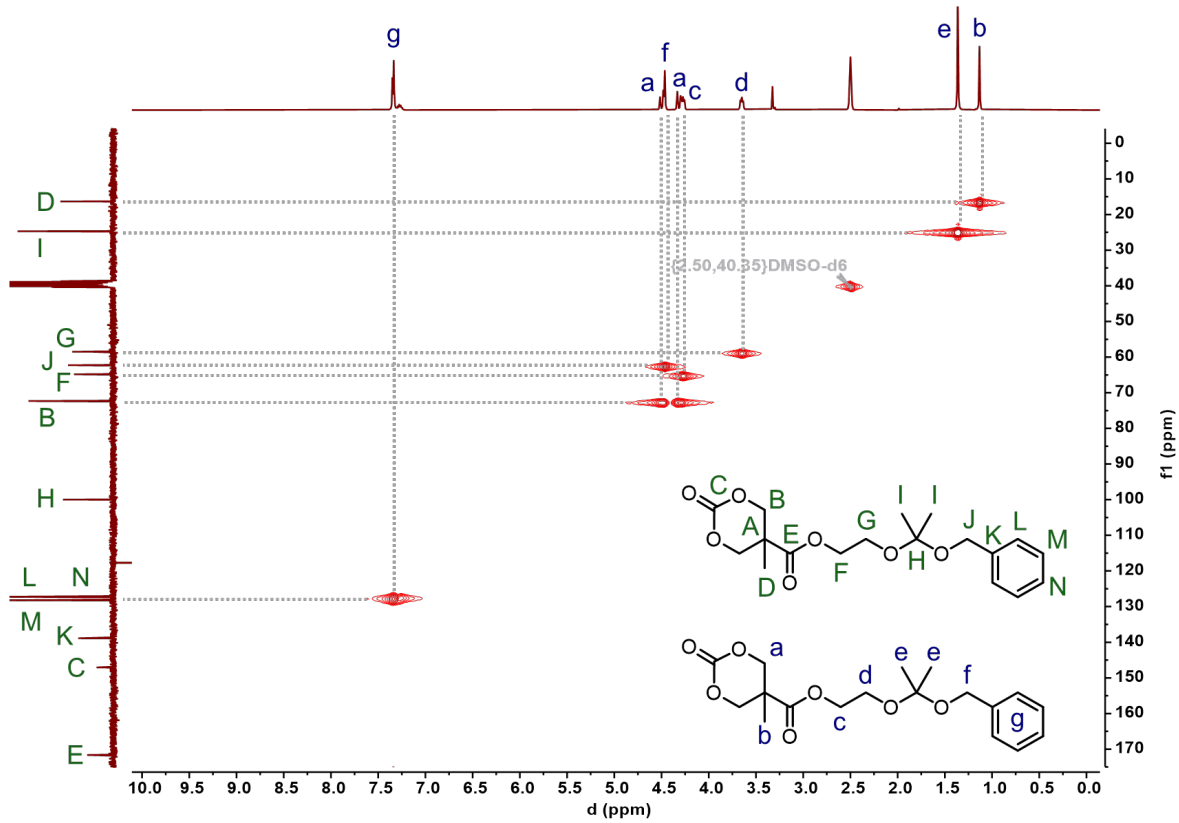

Figure S 25: 2D ^{1}H,^{13}C-HSQC spectrum (DMSO-d_6) of 2-((2-(benzyloxy)propan-2-yl)oxy)ethyl 5-methyl-2-oxo-1,3-dioxane-5-carboxylate (MTC-OEtKBn, **14**).

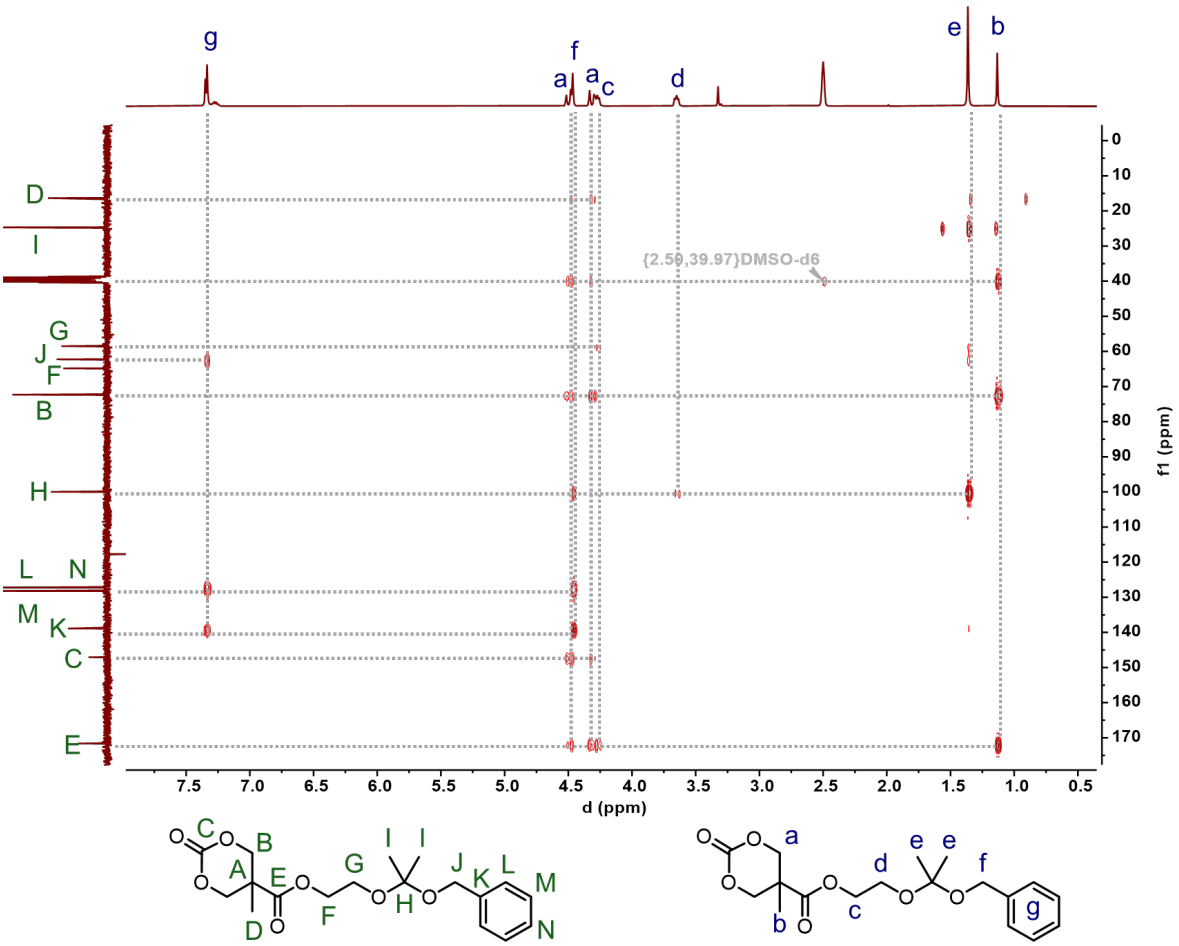

Figure S26: 2D $^{1}H,^{13}C$ HMBC spectrum (DMSO-d_6) of 2-((2-(benzyloxy)propan-2-yl)oxy)ethyl 5-methyl-2-oxo-1,3-dioxane-5-carboxylate (MTC-OEtKBn, **14**).

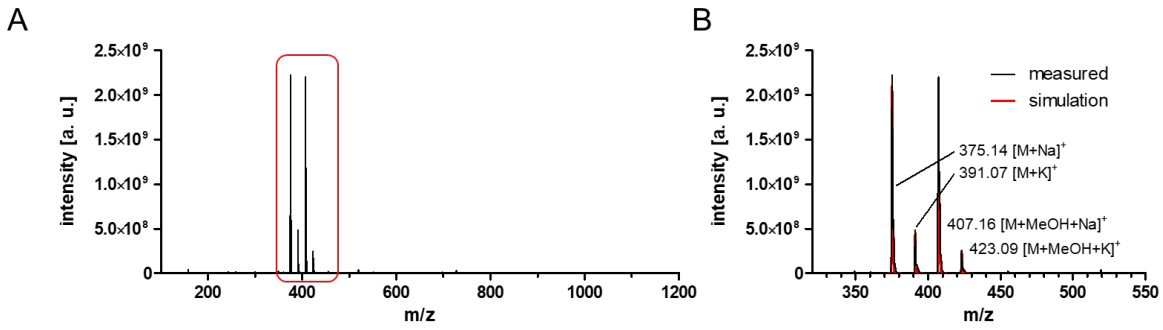

Figure S27: ESI-MS of 2-((2-(benzyloxy)propan-2-yl)oxy)ethyl 5-methyl-2-oxo-1,3-dioxane-5-carboxylate (MTC-OEtKBn, **14**). **A**: Full spectrum with red box marking the magnified are in **B**: K^+ and Na^+ ionized peak flying with and without methanol and corresponding simulations in red.

Crystal Structure Determination

The crystal data of 2-((2-(benzyloxy)propan-2-yl)oxy)ethyl 5-methyl-2-oxo-1,3-dioxane-5-carboxylate (MTC-OEtKBn, **14**) were collected on a RIGAKU XTALAB SYNERGY-R diffractometer with a HPA area detector and multi-layer mirror monochromated $Cu_{K\alpha}$ radiation. The structure was solved using intrinsic phasing method (SHELXT, G. Sheldrick, *Acta Cryst.*, **2015**, *A71*, 3–8), refined with the SHELXL program (G. Sheldrick, *Acta Cryst.*, **2008**, *A64*, 112–122) and expanded using Fourier techniques. All non-hydrogen atoms were refined anisotropically.

Crystal data for MTC-OEtKBn (**14**): $C_{18}H_{24}O_7$, Mr = 352.37, clear colorless plate, 0.250×0.220×0.040 mm^3, orthorhombic space group *Pbca*, a = 11.30(5) Å, b = 12.65(4) Å, c = 24.31(5) Å, V = 3476(20) Å^3, Z = 8, ρ_{calcd} = 1.347 g·cm^{-3}, μ = 0.866 mm^{-1}, $F(000)$ = 1504, T = 100(2) K, R_1 = 0.0327, wR_2 = 0.0798, 3452 independent reflections [$2\theta \leq 149.648°$] and 229 parameters.

Crystallographic data will be deposited with the Cambridge Crystallographic Data Center as supplementary publication no. CCDC-2371836. These data can be obtained free of charge from The Cambridge Crystallographic Data Centre via www.ccdc.cam.ac.uk/data_request/cif.

Table S1: Crystal structure parameters of MTC-OEtKBn (**14**).

Data	**MTC-OEtKBn (14)**
Empirical formula	$C_{18}H_{24}O_7$
Formula weight (g·mol^{-1})	352.37
Temperature (K)	100(2)
Radiation, λ (Å)	$Cu_{K\alpha}$, 1.54184
Crystal system	orthorhombic
Space group	*Pbca*
Unit cell dimensions	
a (Å)	11.30(5)
b (Å)	12.65(4)
c (Å)	24.31(5)
α (°)	90
β (°)	90
γ (°)	90
Volume (Å^3)	3476(20)
Z	8
Calculated density (Mg·m^{-3})	1.347
Absorption coefficient (mm^{-1})	0.866
F(000)	1504
Theta range for collection	3.636 to 74.824°
Reflections collected	31630
Unique reflections	3452
Minimum/maximum transmission	0.645/1.000
Refinement method	Full-matrix least-squares on F^2
Data / parameters / restraints	3452 / 229 / 0
Goodness-of-fit on F^2	1.056
Final R indices [$I>2\sigma(I)$]	R_1 = 0.0316, wR_2 = 0.0790
R indices (all data)	R_1 = 0.0327, wR_2 = 0.0798
Maximum/minimum residual electron density (e·Å^{-3})	0.262 / –0.215

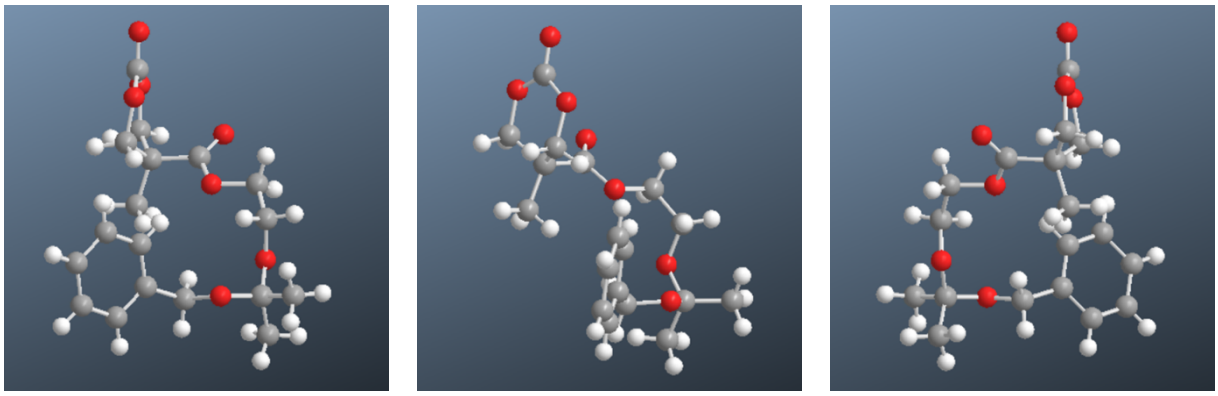

Figure S28: Obtained molecular structure of MTC-OEtKBn (**14**) from three different perspectives, derived by the crystal structure data of Table S1.

POLYMERIZATION

Homopolymer Synthesis

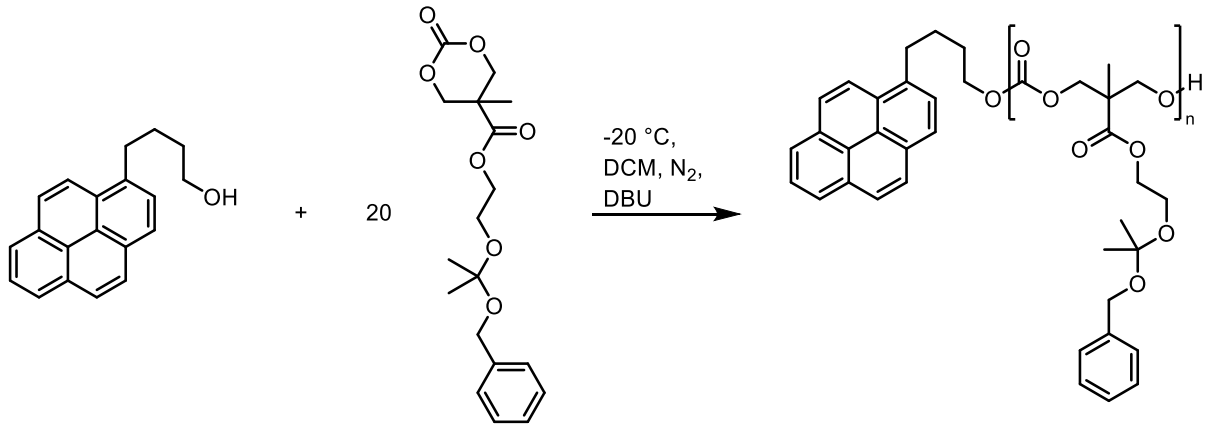

15 **14** **16**

Two 10 mL Schlenk flasks were filled with monomer (**14**) (141.0 mg, 0.40 mmol, 20 eq) and 1-pyrenebutanol (PB, **15**) as initiator (5.5 mg, 0.02 mmol, 1.0 eq), respectively. Both compounds were dried azeotropically with 1 mL benzene by evaporating benzene/water under reduced pressure. To ensure complete removal of water, the drying process was conducted five times. Subsequently, monomer and initiator were each dissolved in dry DCM (800 mL, 600 mL or 400 mL). The solutions were cooled to -20 °C. DBU (2.99 µL, 0.02 mmol, 1.0 eq), which was dried over calcium hydride in advance, was added to the initiator solution. The monomer solution was added to the initiator solution under nitrogen stream. The reaction turnover was monitored by regularly measuring ^{1}H NMR spectra of the reaction mixture. The reaction was quenched at a monomer conversion of 73% by precipitating the homopolymer (**16**) in *n*-hexane at -20 °C. The precipitated polymer was isolated by centrifugation (4000 rpm, 0 °C, 20 min). For purification, the polymer was redissolved in DCM, precipitated in *n*-hexane and isolated by centrifugation two more times. The clean homopolymer (**16**) was dried under reduced pressure yielding a highly viscous colorless liquid(95.2 mg, 88%).

^{1}H NMR (300 MHz, DMSO-d$_6$) δ[ppm]: 8.33–7.91 (m, pyrene-*H*); 7.31–7.22 (m, 5H, Ar-*H*); 4.44–4.38 (m, 2H, Ar-C*H*$_2$-); 4.23–4.11 (m, 6H, pyrene-(CH$_2$)$_4$-O-(C=O)-O-C*H*$_2$-C-C*H*$_2$-, Ar-CH$_2$-O-C-O-CH$_2$-C*H*$_2$-); 3.59–3.54 (m, 2H, Ar-CH$_2$-O-C-O-C*H*$_2$-); 1.79–1.73 (m, pyrene-CH$_2$-(C*H*$_2$)$_2$-); 1.33–1.26 (m, 6H, Ar-CH$_2$-O-(C-(C*H*$_3$)$_2$)-); 1.13–1.03 (m, 3H, pyrene-(CH$_2$)$_4$-O-(C=O)-O-CH$_2$-C-C*H*$_3$).

GPC^{UV} (THF, PS calibration): M_n = 3804 g/mol, $Đ$ = 1.14.

GPC^{RI} (THF, PS calibration): M_n = 4398 g/mol, $Đ$ = 1.22.

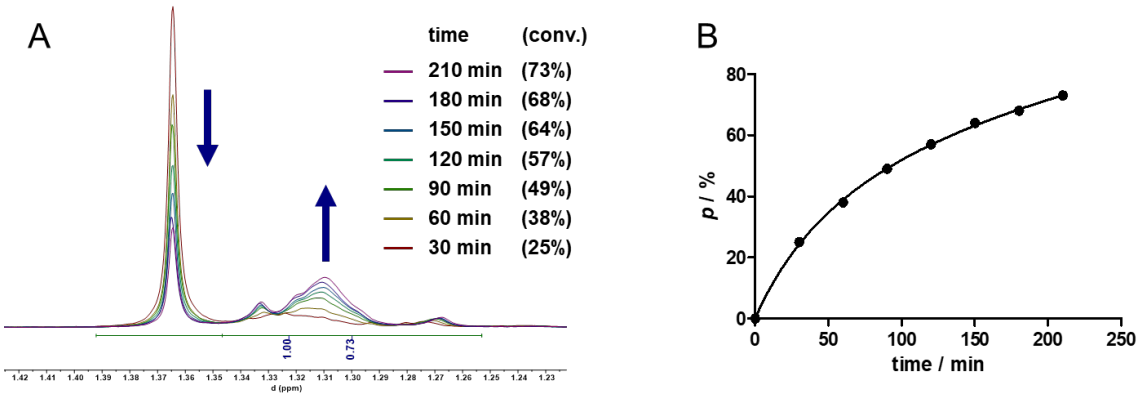

Figure S29: A: Monomer conversion determination by ^{1}H NMR spectroscopy normalizing the methylene groups signal and analyzing the fraction integrated into the polymers backbone. **B**: Polymerization plot of conversion *p* against time *t* for the homopolymerization (the last value is considered an outlier).

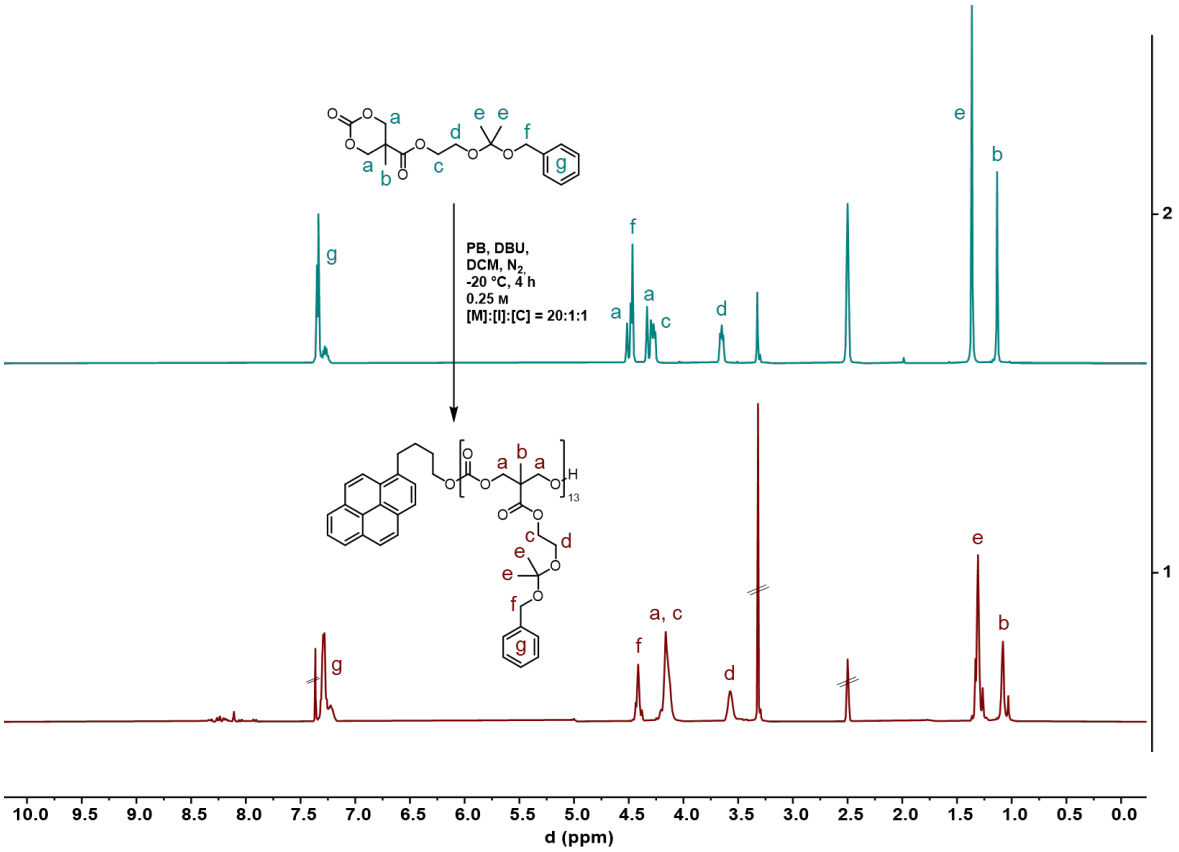

Figure S 30: ^{1}H NMR spectrum (stacked, 300 MHz, DMSO-d_6) of monomer MTC-OEtKBn (**14**) and PB-p(MTC-OEtKBn)$_{13}$ (**16**) with assigned polymer signals.

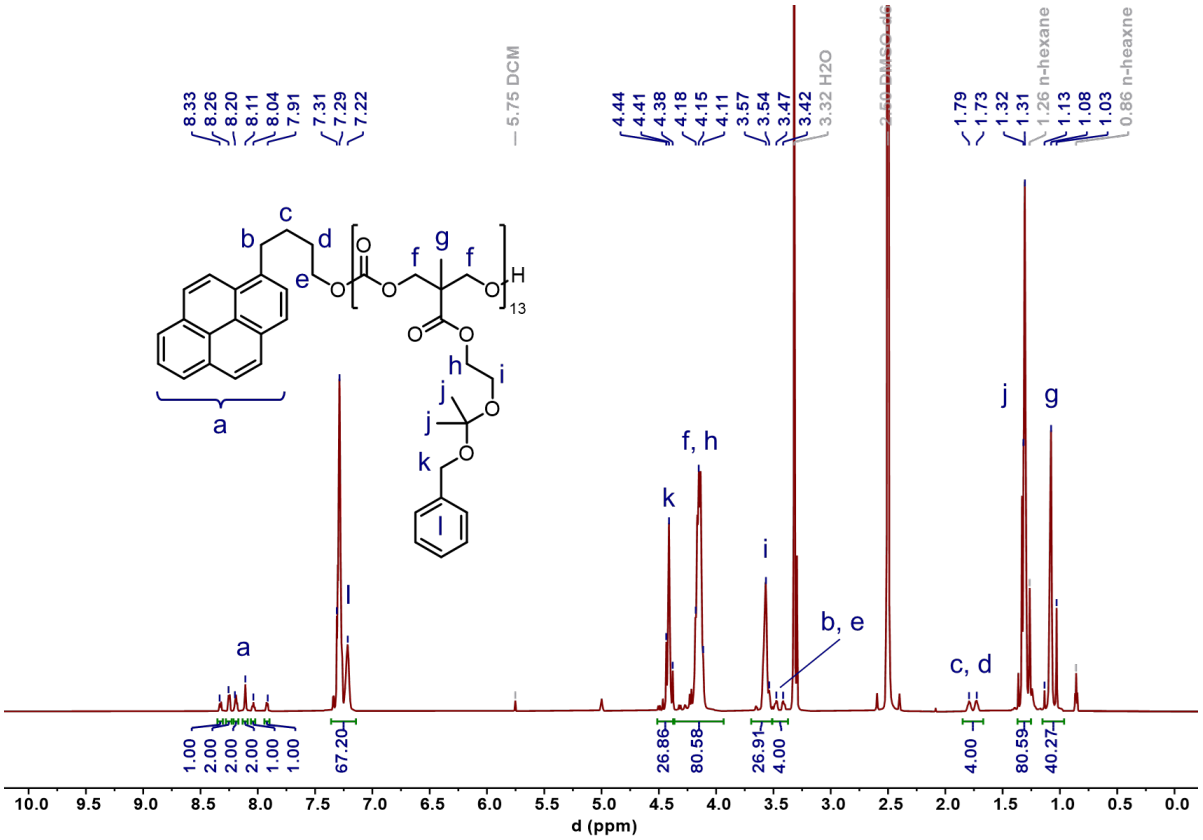

Figure S31: ^{1}H NMR spectrum (300 MHz, DMSO-d_6) of PB-p(MTC-OEtKBn)$_{13}$ (**16**).

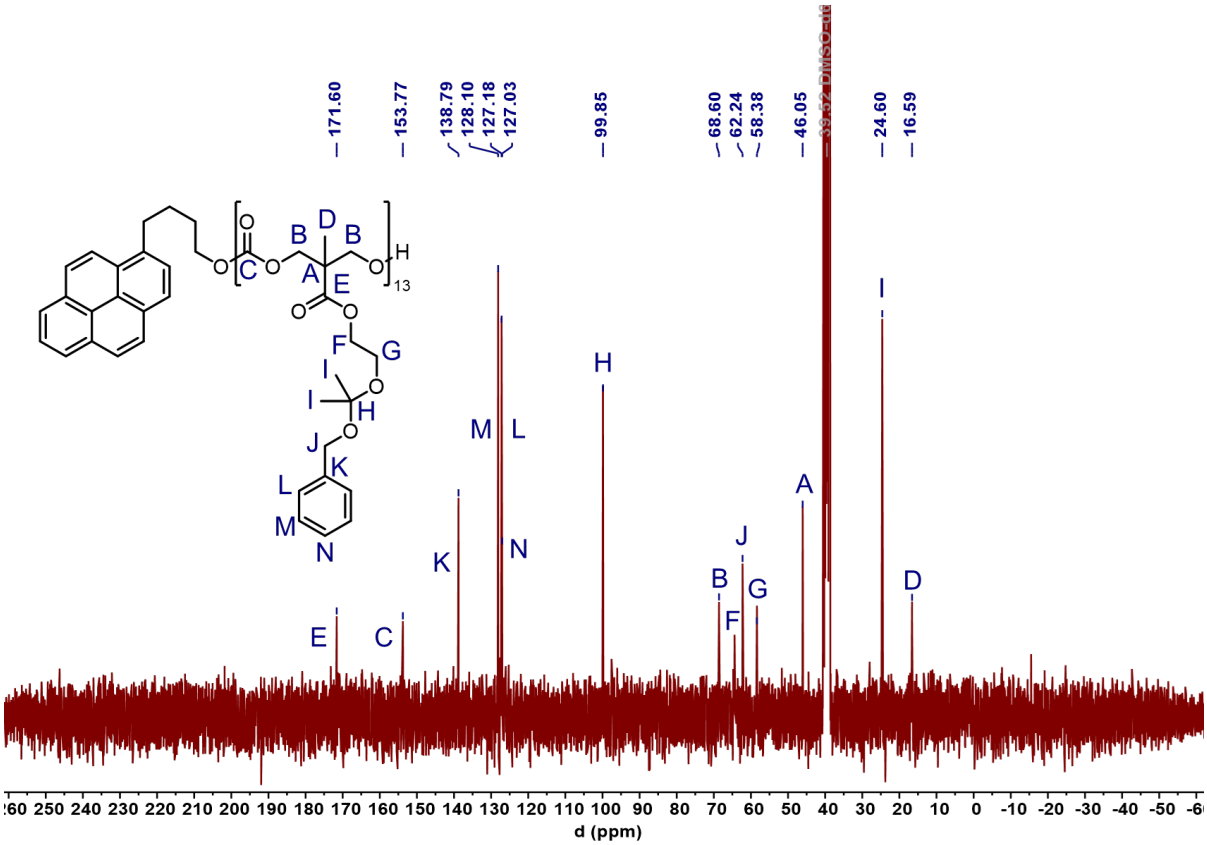

Figure S32: ^{13}C NMR spectrum (175 MHz, DMSO-d_6) PB-p(MTC-OEtKBn)$_{13}$ (**16**).

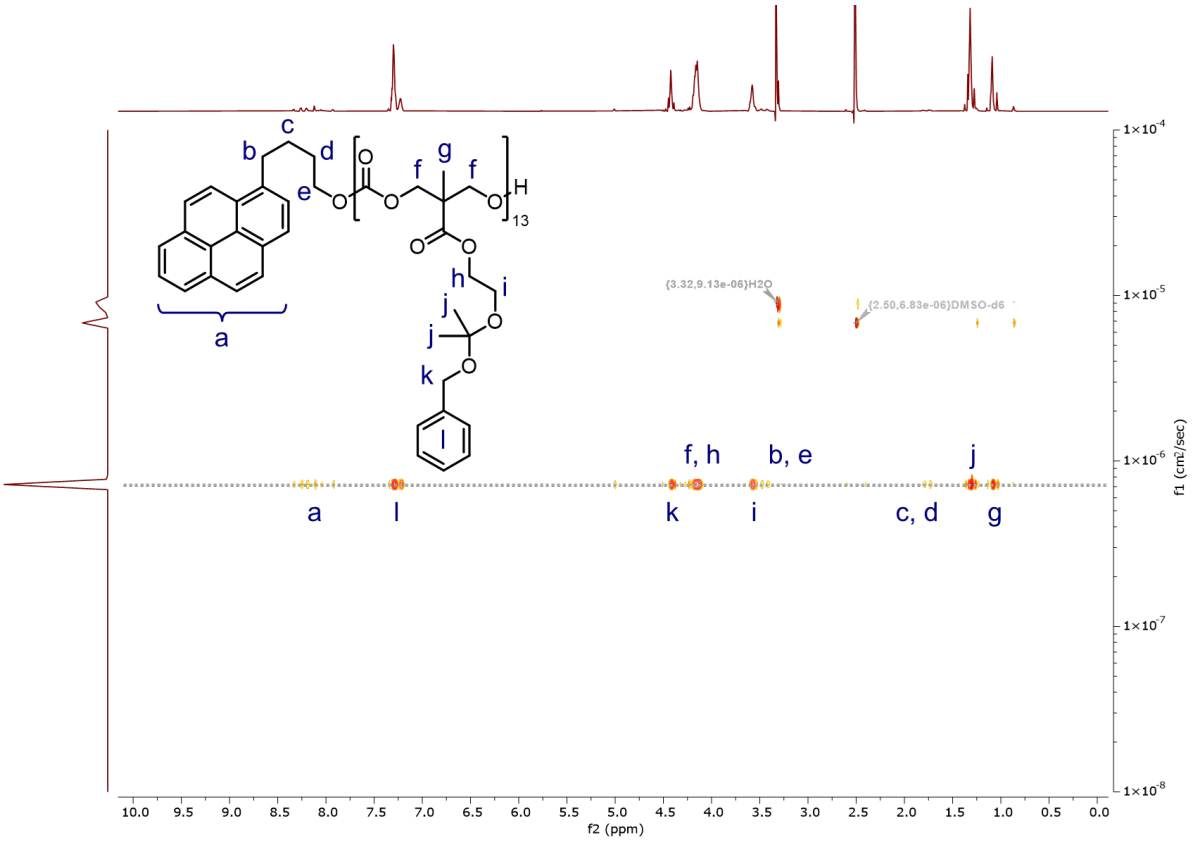

Figure S33: Diffusion ordered ^{1}H NMR spectrum (DMSO-d_6) of PB-p(MTC-OEtKBn)$_{13}$ (**16**).

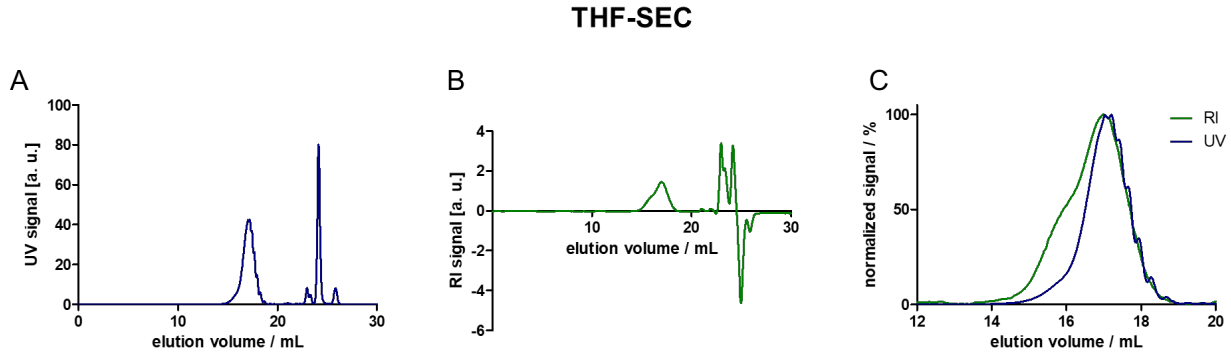

Figure S34: THF-SEC analysis of PB-p(MTC-OEtKBn)$_{13}$ (**16**) **A**: UV-traces and B: RI-traces of PB-p(MTC-OEtKBn)$_{13}$ (**16**). **C**: Section of the overlayed normalized UV- (blue) and RI-signal (green) of the polymer peak.

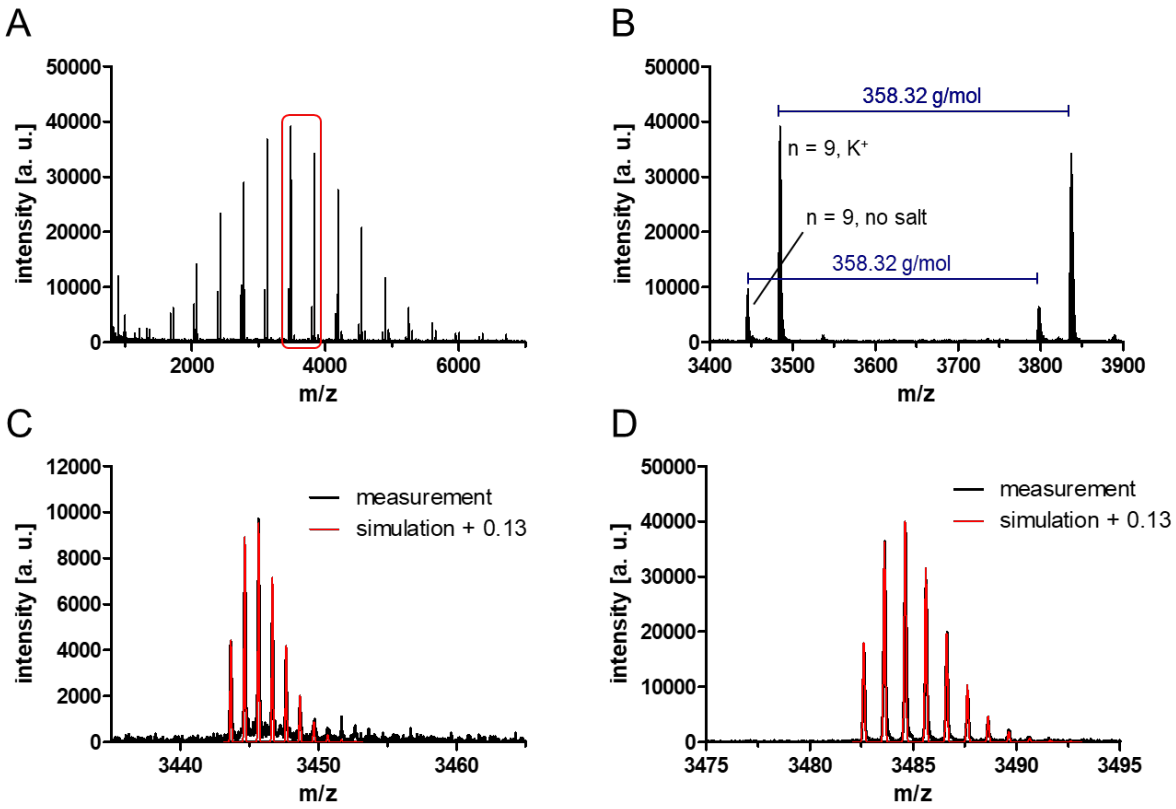

Figure S35: MALDI-ToF mass analysis of PB-p(MTC-OEtKBn)$_{13}$ (**16**). **A**: Full mass spectrum with red box marking the zoomed in area displayed in **B** (including peak assignments and peak distances according to the repeating units molecular weight). **C**: Zoomed in peak with no salt, overlayed with simulation (+0.13 m/z). **D**: Zoomed in peak with K^+ cationized, overlayed with simulation (+0.13 m/z).

Acidic Degradation of Homopolymer

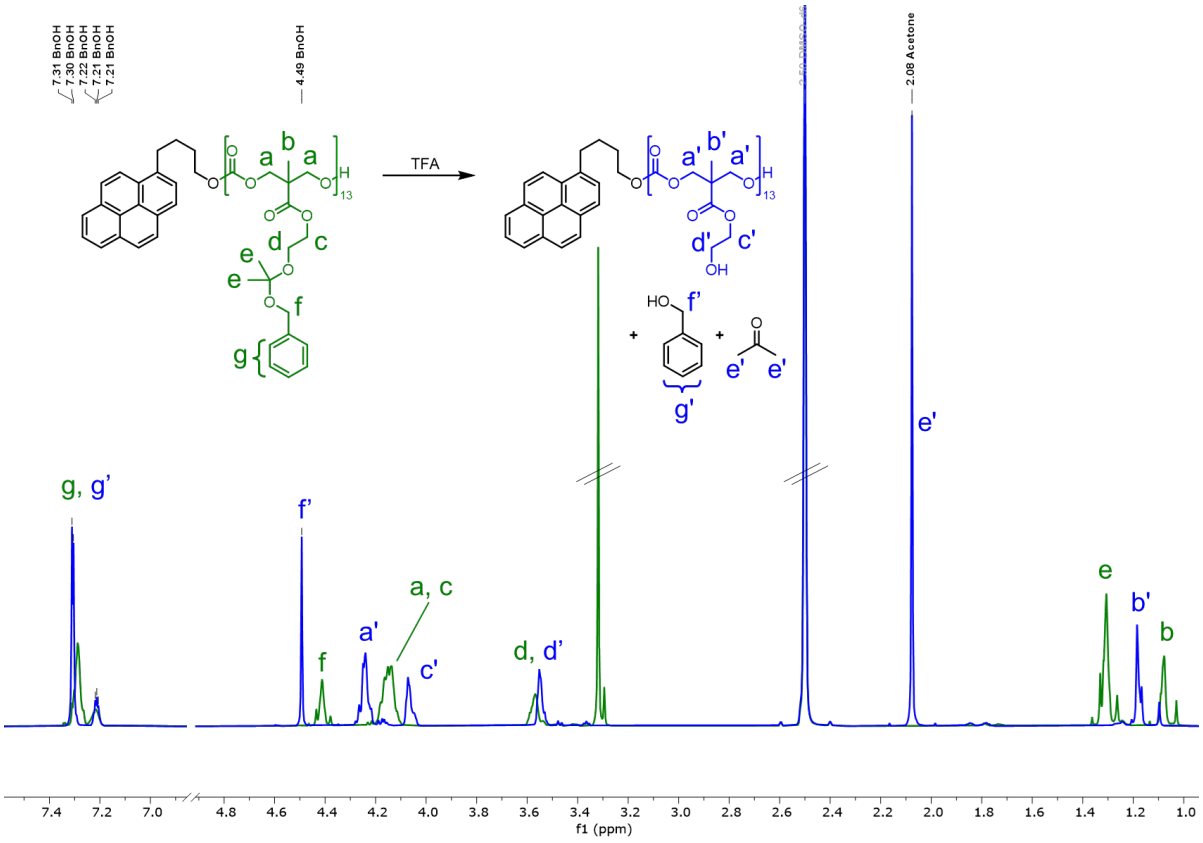

Figure S36: ^{1}H NMR spectrum (superposition, 700 MHz, DMSO-d_6) of PB-p(MTC-OEtKBn)$_{13}$ (**16**) before (green) and after (blue) addition of TFA.

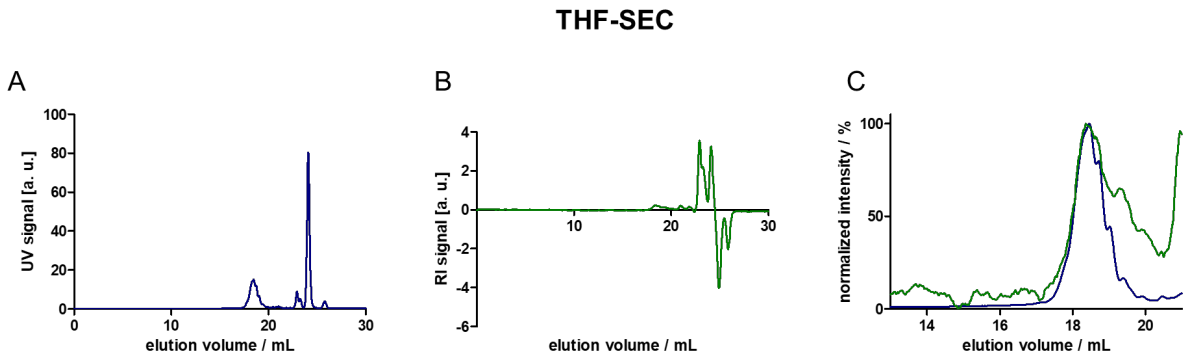

Figure S37: THF-SEC analysis of PB-p(MTC-OEtOH)$_{13}$ **A**: UV-traces and B: RI-traces of PB-p(MTC-OEtOH)$_{13}$. **C**: Section of the overlayed normalized UV- (blue) and RI-signal (green) of the polymer peak. The quality loss in the RI trace is supposed to be the result of an altered refractive index, caused by the transition from a hydrophobic homopolymer into a hydrophilic homopolymer.

Block Copolymer Synthesis

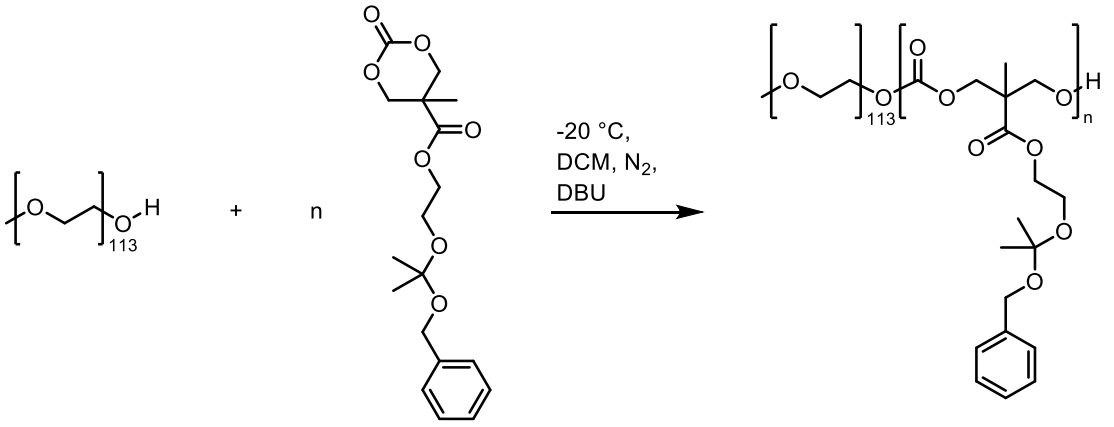

17 **14** **18**

Two 10 mL Schlenk flasks were filled with monomer (**14**) (277.6 mg, 0.79 mmol, 30 eq) and $mPEG_{113}$-OH (**17**) as macro-initiator (131.3 mg, 0.026 mmol, 1.0 eq), respectively. Both compounds were dried azeotropically with 1 mL benzene by evaporating benzene/water under reduced pressure. To ensure complete removal of water, the drying process was repeated four times. Monomer and initiator were each dissolved in 1580 mL dry DCM. The solutions were cooled to -20 °C. Dry DBU (3.92 µL, 0.026 mmol, 1.0 eq) was added to the macro-initiator solution. Subsequently, the monomer solution was added to the macro-initiator solution under a stream of nitrogen. The reaction turnover was monitored by regularly measuring turnover ^{1}H NMR spectra. The reaction was quenched at a conversion of 89% by precipitating the block copolymer in *n*-hexane at -20 °C. The precipitated polymer was isolated by centrifugation (4000 rpm, 0 °C, 20 min). In order to purify the block copolymer, it was re-dissolved in DCM, precipitated in *n*-hexane and isolated by centrifugation two times. Subsequently, the isolated product was dried under reduced pressure, yielding a waxy colorless solid (383.6 mg, 101%). In order to separate homopolymer side product, collected polymer was re-dissolved in DCM, precipitated in Et_2O and isolated by centrifugation three times. The isolated block copolymer (**18**) was dried under reduced pressure (226.0 mg, 60%). The separated ether phase was concentrated under reduced pressure yielding homopolymer side product (149.5 mg, 40%).

^{1}H NMR (300 MHz, DMSO-d_6) δ [ppm]: 7.29–7.23 (m, 5H, Ar-*H*); 4.43–4.42 (m, 2H, Ar-C*H*$_2$-); 4.17–4.15 (m, 6H, $mPEG_{114}$-O-(C=O)-O-C*H*$_2$-C-C*H*$_2$-, Ar-CH_2-O-C-O-CH_2-C*H*$_2$-); 3.58 (m, 2H, Ar-CH_2-O-C-O-C*H*$_2$-); 3.51 (m, mPEG-*H*); 3.24 (s, CH_3-PEG); 1.33–1.32 (m, 6H, Ar-CH_2-O-(C-(C*H*$_3$)$_2$)-); 1.11–1.03 (m, 3H, $mPEG_{114}$-O-(C=O)-O-CH_2-C-C*H*$_3$).

GPC^{UV} (THF, PS calibration): M_n = 9260 g/mol, $Đ$ = 1.05.

GPC^{RI} (THF, PS calibration): M_n = 8514 g/mol, $Đ$ = 1.05.

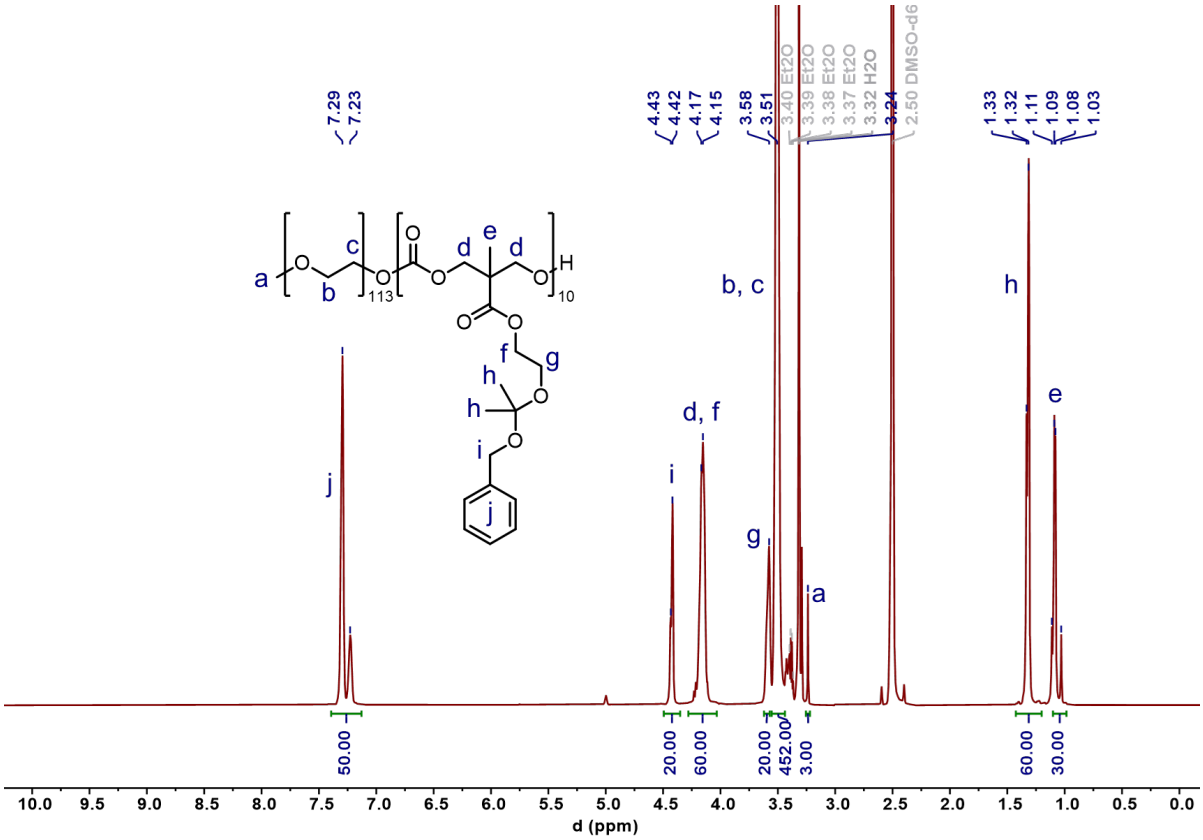

Figure S38: ^{1}H NMR spectrum (300 MHz, DMSO-d$_6$) of mPEG-*b*-p(MTC-OEtKBn)$_{10}$ (**18**).

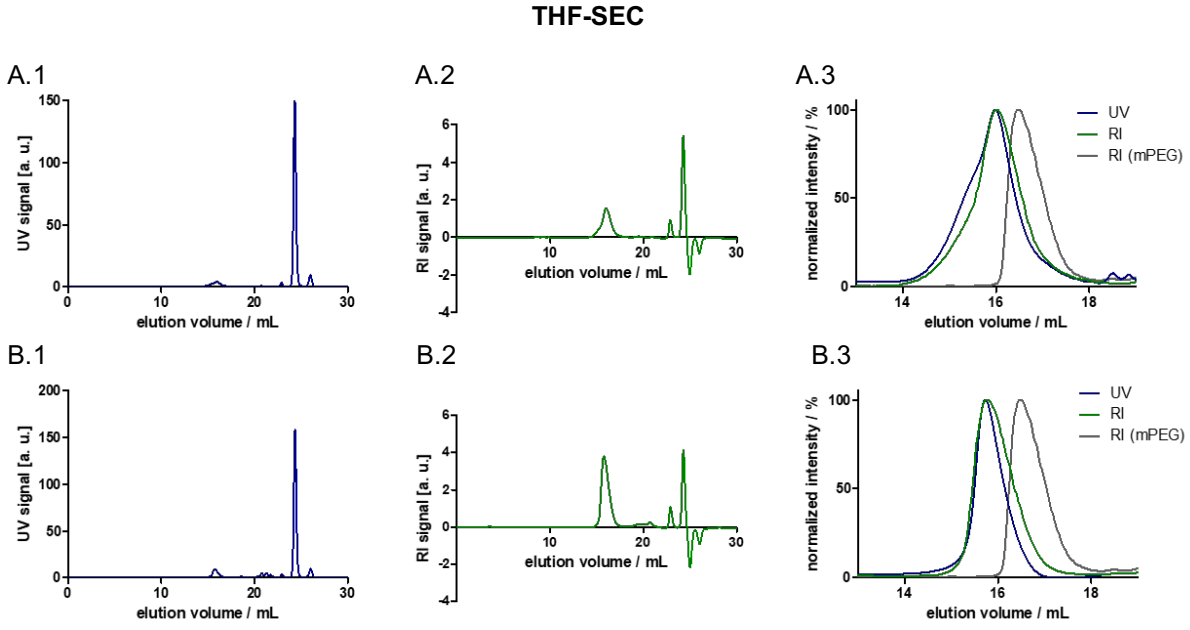

Figure S39: THF-SEC analysis of mPEG-*b*-p(MTC-OEtKBn)$_{10}$ (**18**). **A**: Analysis after precipitation in *n*-hexane. **A.1**: UV-traces and **A.2**: RI-traces of product mixture. **A.3**: Section of the overlayed normalized UV- (blue) and RI-signal (green) of the polymer peak next to the mPEG macro-initiator signal (grey). **B**: Analysis after precipitation in Et$_2$O. **B.1**: UV-traces and **B.2**: RI-traces of mPEG-*b*-p(MTC-OEtKBn)$_{10}$ (**18**). **B.3**: Section of the overlayed normalized UV- (blue) and RI-signal (green) of the polymer peak next to the mPEG macro-initiator signal (grey).

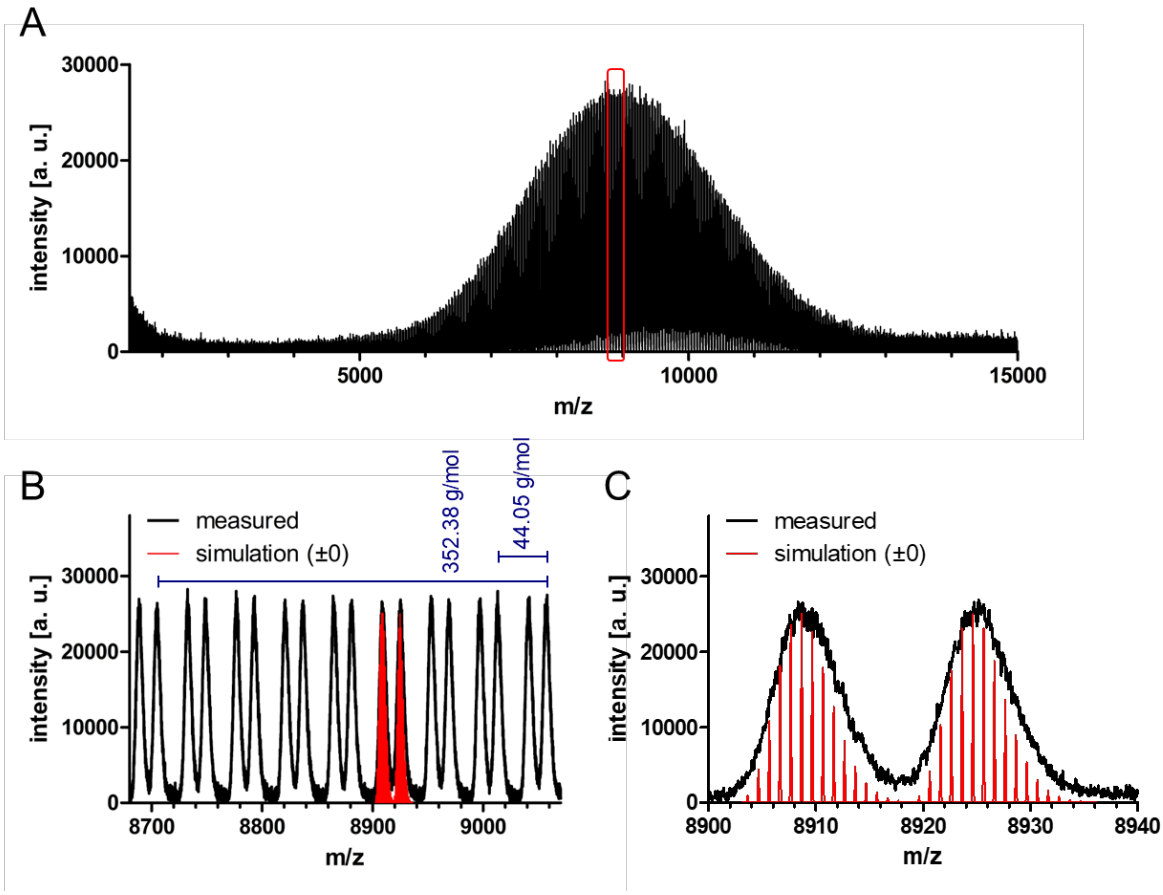

Figure S40: MALDI-ToF mass spectrometry analysis of mPEG-*b*-p(MTC-OEtKBn)$_{10}$ (**17**). **A**: Full mass spectrum with red box marking the zoomed in area displayed in **B** (including peak distances according to both repeating units molecular weight). **C**: Zoomed in mPEG$_{113}$-*b*-p(MTC-OEtKBn)$_{11}$ peak with with K^+ cationized and Na^+ cationized, overlayed with simulation (±0 m/z).

POLYMERIC MICELLE FORMULATION

Solvent evaporation method

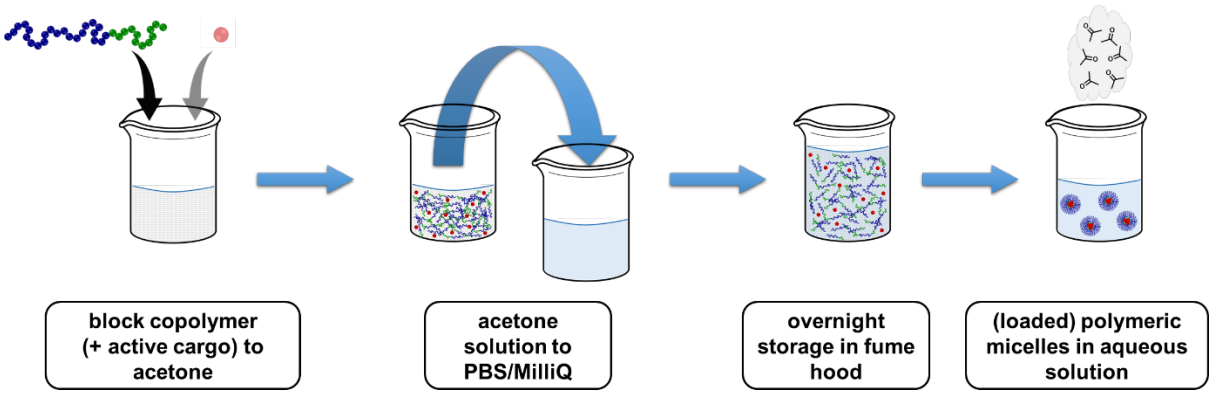

Scheme S1: Schematic illustration of the solvent evaporation method for the formulation of polymeric micelles.

To formulate polymeric micelles from the synthesized block copolymers, the solvent evaporation method introduced by Bagheri et al. was used.[4] 5.5 mg of mPEG-*b*-p(MTC-OEtKBn)$_{10}$ was dissolved in 1.1 mL acetone (p. A.). 1.0 mL of this acetone solution was added to 1.0 mL TRIS buffer in a tared snap cap vial. The open vial was overnight stored in the fume hood to allow the acetone to evaporate. The complete evaporation of acetone was confirmed by weighting the snap cap vial. Evaporated water was refilled with DI water, and the solution was filtered through a syringe filter (macherey-nagel, 0.45 µm pore size, H-PTFE membrane). The micelles size distribution and poly dispersity index were analyzed by DLS.

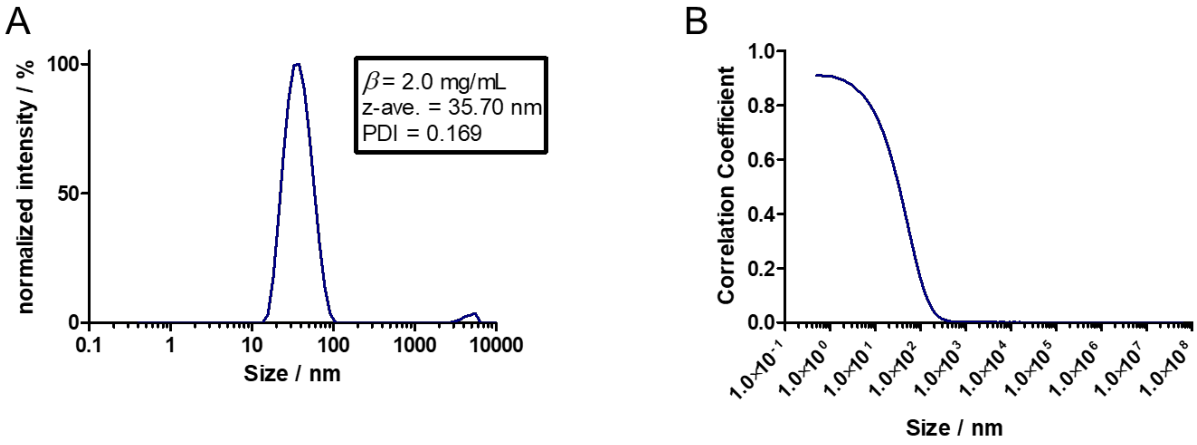

Figure S 41: DLS analysis of polymeric micelles in TRIS buffer (pH = 7.4) formulated with the solvent evaporation method. **A**: Normalized intensity plot of the micelles size distribution and **B**: the corresponding correlogram.

Transmission electron microscopy (TEM) imaging

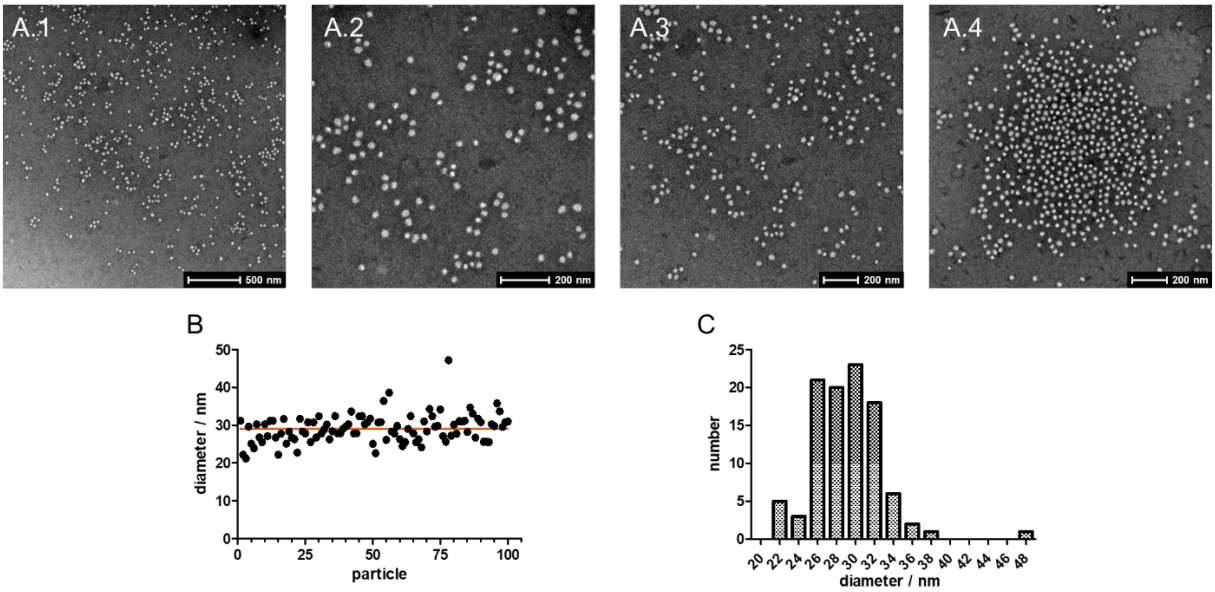

Figure S42: A.1–4: Selection of TEM pictures of polymeric micelles, formulated from $mPEG_{113}$-*b*-p(MTC-OEtKBn)$_{10}$. **B**: Diameters of 100 randomly evaluated particles and their average size (red line). **C**: Histogram of these particle sizes.

Acidic degradation study of polymeric micelles

To formulate polymeric micelles in other buffers than PBS, a high concentrated micelle stock solution was prepared. 11.0 mg of mPEG-*b*-p(MTC-OEtKBn)$_{13}$ were dissolved in 1.1 mL acetone (p. A.). 1.0 mL of this acetone solution were added to 1.0 mL DI water in a tared snap cap vial. The open vial was overnight stored in the fume hood to allow the acetone to evaporate. The complete evaporation of acetone was confirmed by weighting the snap cap vial. Evaporated water was refilled with DI water, and the solution was filtered through a syringe filter (macherey-nagel, 0.45 µm pore size, H-PTFE membrane). Subsequently 0.1 mL of the high concentrated stock solution was diluted into 0.9 mL of the desired buffer (acetate buffer or PBS at an adjusted pH level) respectively achieving a final micelle concentration of 1.0 mg/mL.

After diluting the micelle solutions into the buffers, DLS measurements were performed repeatedly over a period of 56 d. The declining derived count rate was used as evidence of the micelle degradation. Additionally, the change of the nanoparticles size distribution in acidic environments indicated micelle degradation.

Table S2: Half-life of polymeric micelles at different pH levels.

pH	$t_{1/2}$ / h	$t_{1/2}$ / d
6.0	177.8	7.41
5.5 (PBS)	67.11	2.80
5.5 (ac.)	62.02	2.58
5.0	17.40	0.725
4.5	4.457	0.186
4.0	1.563	0.0651
3.6	0.7217	0.0301

Nile red release study

To encapsulate nile red in the polymeric micelles, the previously described solvent evaporation method was extended by dissolving the hydrophobic dye together with the block copolymer in acetone (p. A.). The formulated micelles were diluted into PBS (pH 7.4), acetate buffer (pH 5.5) and ammonia buffer (pH 9.5) respectively ending up with a block copolymer mass concentration of 2.0 mg/mL. Immediately after diluting the micelles into the buffers, the three samples were analyzed by DLS and UV/vis spectroscopy.

Critical Micelle Concentration (CMC)

To determine the critical micelle concentration (CMC), polymeric micelles were formulated according to the solvent evaporation method but with 0.6 µM pyrene dissolved in acetone in prior. After the formulation process, a dilution series of the polymeric micelles was prepared (4.0 – 0.00004 mg/mL) in PBS which also contained 0.6 µM pyrene. 200 µL of each concentration were added to a black 96 well plate (thermoscientific Nucleon™ Delta Surface) in triplicates and the pyrene fluorescence was detected using a plate reader (ex.: 333 nm, bw.: 5.0 nm; em.: 360–460 nm bw: 5.0 nm). The ratio of I_3 (384 nm) and I_1 (373 nm) fluorescence bands were plotted against the decadic logarithm of the polymer concentration, and linear regimes were found for small, medium and large polymer concentrations. The intersection of the linear regression line of the small concentration regime and the medium concentration regime were calculated, giving a CMC of 131 nmol/L.

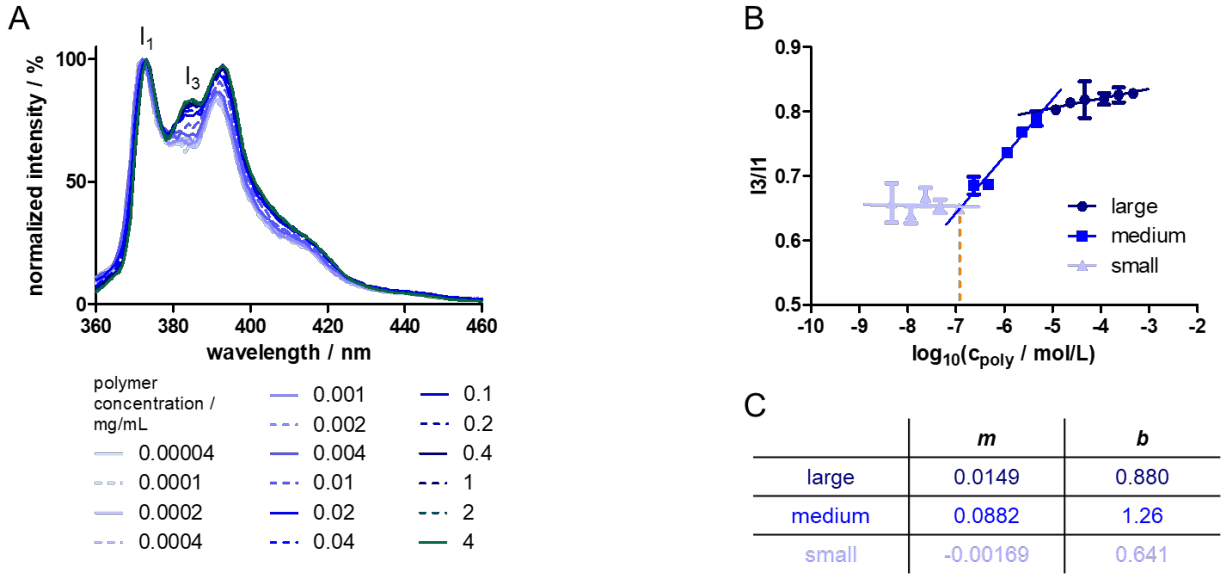

	m	*b*
large	0.0149	0.880
medium	0.0882	1.26
small	-0.00169	0.641

Figure S 43: A: Fluorescence spectrum of pyrene encapsulated in $mPEG_{113}$-b-$p(MTC\text{-}OEtKBn)_{10}$ at a polymer concentration of 4.0 mg/mL together with the fluorescence spectra of the diluted polymer samples (2.0–0.00004 mg/mL) normalized to the I_1 fluorescence band. Encapsulated pyrene leads to an increased I_3 fluorescence band. In the absence of micellar structures, pyrene is present in the hydrophilic environment of the solvent, leading to a decline of the I_3 fluorescence band. **B**: Ratio of I_3 and I_1 fluorescence band plotted against the decadic logarithm of the polymer concentration. Linear regimes can be observed for a small, medium and large polymer concentration regime, which can be fitted by three regression lines. The slope *m* and y-axis intersection *b* of these regression lines are given in **C**. The intersection of the regression line of the small and the medium polymer concentration regime gives the CMC (131 nmol/L).

$$0.0882 \log(c_{poly}) + 1.26 = -0.00169 \log(c_{poly}) + 0.641$$

$$loc(c_{poly}) = -6.88$$

$$CMC = 10^{-6.88} \frac{\text{mol}}{\text{L}} = 0.131 \cdot 10^{-6} \frac{\text{mol}}{\text{L}}$$

Flow Cytometry (FC)

To investigate the cellular uptake of polymeric micelles formulated from mPEG-*b*-p(MTC-OEtKBn)$_{10}$ by macrophages, Rhodamine b octadecyl ester perchlorate (Rhodamine C18) loaded micelles were formulated. For this purpose, 1.1 mg mPEG-*b*-p(MTC-OEtKBn)$_{10}$ were combined with 2.5wt% Rhodamine C18 and dissolved in 1.1 mL acetone. 1 mL of this acetone solution was added to 1 mL PBS in a tared snap cap vial, working at a sterile cell bench. The uncapped vial was overnight stored in the cell bench, allowing the acetone to evaporate. After confirming the complete acetone evaporation by weighting the vial, additionally evaporated water was refilled with millipore water readjusting the block copolymer weight concentration of 1.0 mg/mL. The micelle solution was filtered through a H-PTFE syringe filter (0.45 µm pore size, macherey-nagel). As negative reference, the formulation process was also conducted using dye but in absence of block copolymer. The dye loading was determined by UV/vis absorption spectroscopy. For the dye loaded particles, a dye loading of 0.33 wt% was determined, corresponding to a loading efficiency of 13.2%.

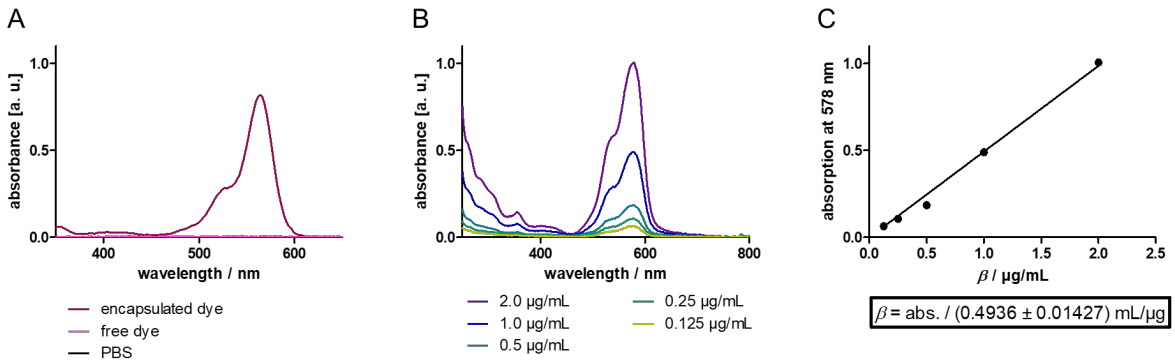

Figure S44: Rhodamine C18 loading determination by UV/vis absorption spectroscopy. **A**: absorption spectrum of dye loaded polymeric micelles, free dye and PBS (revealing the enhanced solubility of the hydrophobic dye by the polymeric micelles). **B**: UV/vis absorption spectra of a concentration series prepared from a Rhodamine C18 DMSO stock solution diluted into PBS. **C**: Calibration line of Rhodamine C18 in PBS and derived linear equation.

A 24-well plate was filled with 900 µL cell suspension per well (235,000 cells per well). The 24-well plate was stored in the incubator (37 °C, 5% CO_2,) for 24 h. To the cell adhered overnight to the well bottom 100 µL of a sterile prepared polymeric micelle solution was added resulting in a final polymeric micelle concentration of 100 µg/mL. The cells were incubated for 16 h. After removing the cell culture medium, the cells were washed with 1 mL PBS per well. Subsequently, 500 µL of dissociation buffer was added to each well and the cells were incubated for 20 min. The detached cells were transferred into an Eppendorf tube and stored on ice. The cells were separated from the dissociation buffer by centrifugation (10 min, 1,000 rpm, 5 °C) and resuspended in 200 µL PBS. Flow cytometry analysis were performed on a BD AccuriTM C6 and BD Fortessa flow cytometer. Data were processed using FlowJo soft-ware package. The measurements were run until 50,000 cells were counted. Each sample was conducted as triplicate (n = 3).

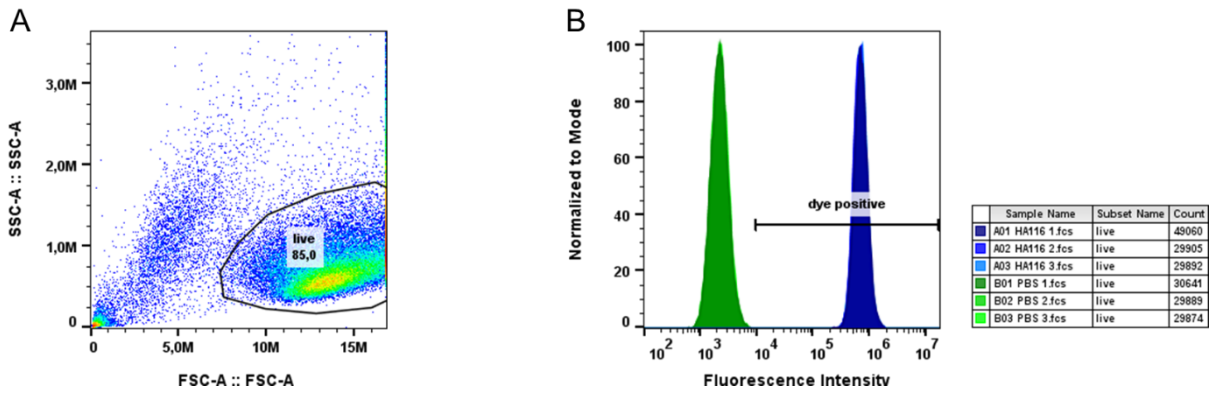

Figure S45: Flow cytometry analysis of macrophages incubated with Rhodamine B octadecyl ester loaded polymeric micelles (blue) or PBS (green). **A**: Gating strategy of flow cytometry of RAW Blue macrophages. **B**: Fluorescence intensity histogram of macrophages incubated with dye loaded polymeric micelles (blue) and PBS incubated macrophages (green).

Confocal Fluorescence Microscopy Imaging

Raw Blue macrophages were seeded into an Ibidi µ-slide eight-well confocal microscopy chamber (50,000 cells/well). The macrophages were suspended in 180 µL cell culture medium and allowed to adhere. After 16 h, the cells were treated with 20 µL of Rhodamine C18-loaded micelle solution in PBS (same samples as used for flow cytometry). The cells were incubated at 37 °C for 24 h. The culture medium was then removed, and the cells were washed with PBS (3 x 200 µl). Subsequently, 200 µl of 4% paraformaldehyde was added and fixed at 37 °C for 15 min. Cells were then washed again with PBS and nuclei were stained by incubation with 150 µL of 4'-6-diamidino-2-phenylindol (DAPI, 50 µg/mL in PBS) for 10 min at 37 °C. Cells were finally washed with PBS and stored in aqueous mounting medium. Confocal fluorescence microscopy images were obtained using a STELLARIS 8 Leica DMi8 confocal microscope (Wetzlar, Germany) with a HC PL APO CS2 40x/1.25 GLYC oil immersion objective. All images were processes by Leica Applcation Suite X 3.7.4.23463 of Leica Microsystem.

Protein aggregation study

For multi angle dynamic light scattering (DLS) experiments of plasma incubated micelles, CL075 loaded polymeric micelles were prepared using the solvent evaporation method under sterile conditions. 2.7 mg mPEG-*b*-p(MTC-OEtKBn)$_{10}$ were combined with 5.0wt% CL075 and dissolved in 0.54 mL acetone. 0.5 mL of this acetone solution were added to 0.5 mL PBS in a tared snap cap vial, working at a sterile cell bench. The uncapped vial was overnight stored in the cell bench, allowing the acetone to evaporate. After confirming the complete acetone evaporation by weighting the vial, additionally evaporated water was refilled with millipore water readjusting the block copolymer weight concentration of 5.0 mg/mL. The micelle solution was filtered through LCR membrane syringe filters (0.45 µm pore size, PALL Life Science). Citrate stabilized human plasma was filtered through GS membrane syringe filters (0.2 µm pore size, PALL Life Science). 400 µl of the plasma was mixed with 100 µl micelle sample into dust free cylindrical scattering cuvettes and incubated at 37 °C for 1 h. The DLS measurements were performed with a Uniphase He/Ne Laser (632.8 nm, 22 mW), an ALV-SP125

Goniometer, an ALV/High QE APD-Avalanche photodiode, an ALV5000/E/PCI-correlator and a Lauda RC-6 thermostat unit. The angular dependent measurements were performed between 30° and 150° in 20° steps. Data analysis was performed according to the procedure described by Rausch et al.[1]

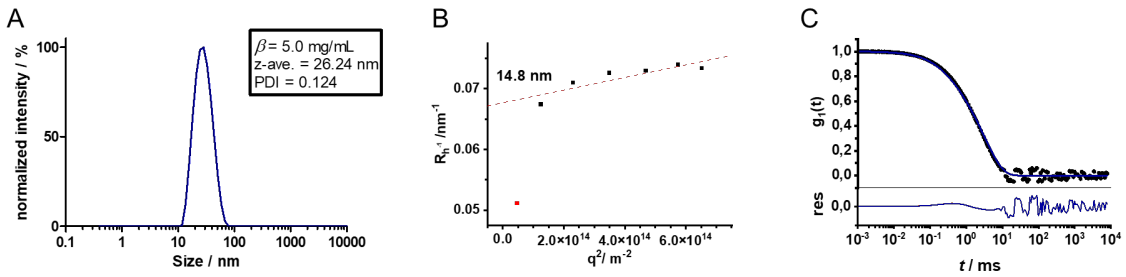

Figure S46:A: Normalized size distribution intensity plot of CL075 loaded polymeric micelles formulated from mPEG-*b*-p(MTC-OEtKBn)$_{10}$ block copolymers analyzed by conventional DLS. **B/C**: Blood plasma aggregation study by multi angle DLS analysis. The determined diameter in **A** can be confirmed by the reciprocal hydrodynamic radius R_H vs. squared scattering vector q^2 plot of these nanoparticles (**B**). **C**: Autocorrelation curve, measured at an angle of 50° for CL075 loaded micelles. The autocorrelation curves were recorded after 1 h incubation in human blood plasma and compared to the sum of autocorrelation curves obtained from individual measurements of plasma and micelles.

IN VITRO PERFORMANCE

To perform cell assays on Raw Blue macrophages, CL075 loaded micelles were formulated by the solvent evaporation methode. For this purpose, 2.75 mg mPEG-*b*-p(MTC-OEtKBn)$_{10}$ block copolymer was dissolved in 1.1 mL acetone (2.5 mg/mL) together with 2wt% CL075 (50 µg). 1.0 mL of this solution was added to 1.0 mL PBS in a tared snap cap vial, working under sterile conditions at a cell bench. The uncapped vial was overnight stored in the cell bench, allowing the acetone to evaporate. After confirming the complete acetone evaporation by weighting the vial, additionally evaporated water was refilled with millipore water readjusting the block copolymer weight concentration of 2.5 mg/mL. The micelle solution was filtered through a H-PTFE syringe filter (0.45 µm pore size, macherey-nagel). Additionally, unloaded micelles and free CL075 without the nanocarrier were formulated following the same procedure. The drug loading was determined by UV/vis spectroscopy.

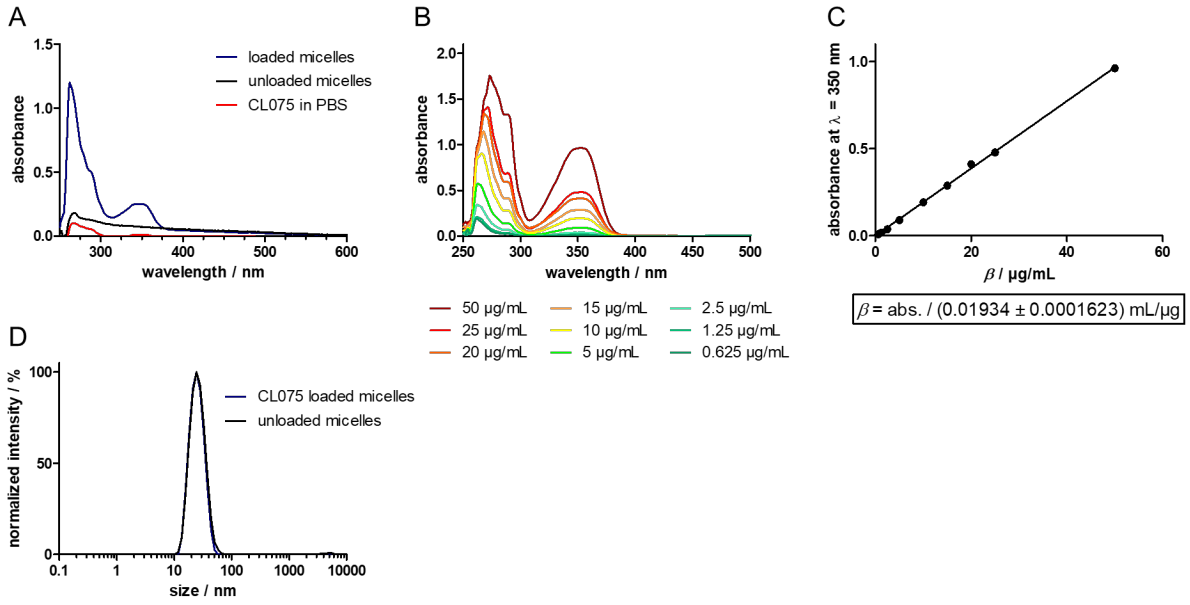

Figure S47: CL075 loading determination by UV/vis absorption spectroscopy. **A**: absorption spectrum of CL075 loaded polymeric micelles (blue), unloaded micelles (black, 48.6 µg/mL, 1.94wt%, 97.2% efficiency) and formulated CL075 (red, 2.58 µg, 5.17% efficiency). **B**: UV/vis absorption spectra of a concentration series prepared from a CL075 stock solution in DMSO. **C**: Calibration line of CL075 in DMSO and derived linear equation. **D**: Normalized size distribution intensity plot of unloaded (black) and CL075 loaded (blue) polymeric micelles analyzed by DLS.

The loaded micelles carried 48.6 µg/mL (199.7 µmol/L) CL075 (48.6 µg, 1.94wt%, 97.2% efficiency), while the PBS was only capable of carrying 2.58 µg/mL (10.62 µmol/L) CL075 (5.17% efficiency).

Based on these results, a dilution series of the loaded micelles was prepared in the range of 199.7 µmol/L to 0.20 µmol/L regarding the CL075 concentration. From the unloaded micelle solution and the free CL075 solution dilution series were prepared using equal amounts as used for the loaded samples. Furthermore, a free CL075 dilution series in cell culture medium, derived from a 25 mg/mL DMSO stock solution, was prepared in the same CL075 concentration range.

RAW-Blue macrophage TLR reporter assay (Quanti Blue Assay)

To perform the Quanti Blue assay, 180 µL cell suspension ($c = 0.5 \cdot 10^6$ cells/mL) were seeded in a 96-well plat (90,000 cells/well). The cells were left to adhere. After overnight incubating (37 °C, 5% CO_2), 20 µL of the previously prepared stock solutions were added to the wells as quartets ($n = 4$). The treated cells were incubated for 24 h. Then, 150 µL Quanti-Blue™ solution was added to each well of a new well plate. To these wells 50 µL supernatant from the cell containing well plates were added. After incubation at 37 °C for 30 min, the readout was performed at a wavelength of 620 nm using a Tecan plate reader.

MTT-Assay

The remaining cells from the QUANTI-Blue™ assay were used for an MTT assay. To these cells 30 µL 3-(4,5-Dimethylthiazol-2-yl)-2,5-diphenyltetrazolium bromide (MTT) solution (2 mg/mL MTT) was added. After incubating at 37 °C for 1 h 100 µL, formed formazan crystals were dissolved by adding 10% SDS/0.01 M HCl solution to each well. After incubating again at 37 °C for 24 h to assure cell lysis and formazan solubilization the readout was performed at a wavelength of 570 nm using a Tecan plate reader.

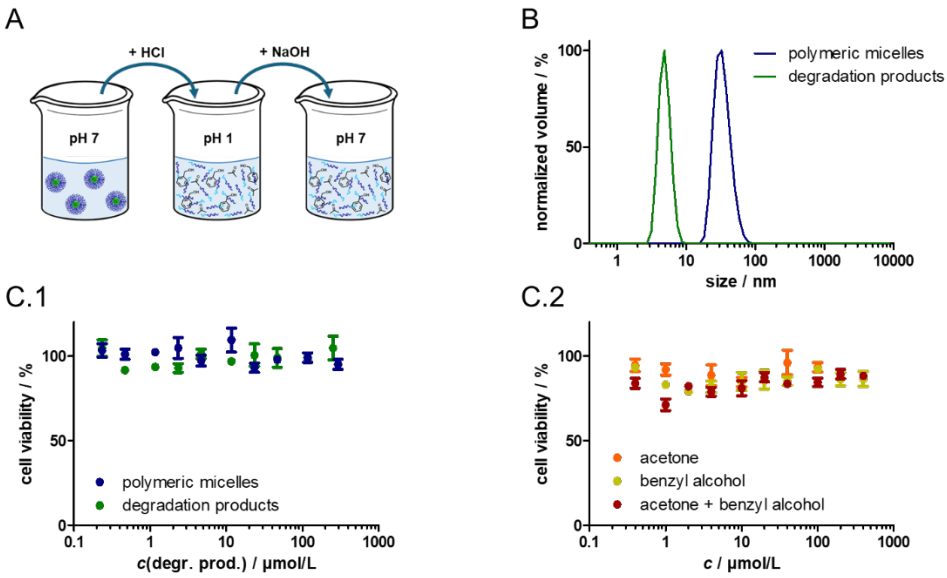

Figure S48: MTT assay of degradation Products **A**: Degrading strategy: polymeric micelles were formulated in PBS and then treated with 10vol% 1M HCl. Subsequently, the solution was neutralized with an equivalent volume of 1M NaOH. **B**: DLS volume plot of the formulated polymeric micelles in PBS next to the degradation products after treatment with HCl. **C.1**: MTT-assay of polymeric micelles and their degradation products. The concentration corresponds to the maximum amount of degradation products that can be formed and is equal to the amount used for the immune stimulation assay. **C.2**: MTT-assay of small molecule fragments acetone and benzyl alcohol, that are formed during the acidic micelle degradation, as well as the combination of both.

LITERATURE

[1] K. Rausch, A. Reuter, K. Fischer, M. Schmidt, *Biomacromolecules* **2010**, *11*, 2836–2839.

[2] R. C. Pratt, F. Nederberg, R. M. Waymouth, J. L. Hedrick, *Chem. Commun.* **2008**, *2*, 114–116.

[3] T. F. Al-Azemi, K. S. Bisht, *Macromolecules* **1999**, *32*, 6536–6540.

[4] M. Bagheri, J. Bresseleers, A. Varela-Moreira, O. Sandre, S. A. Meeuwissen, R. M. Schiffelers, J. M. Metselaar, C. F. Van Nostrum, J. C. M. Van Hest, W. E. Hennink, *Langmuir* **2018**, *34*, 15495–15506.